SPECIFIC RESISTANCE AND SPECIFIC INTENSITY OF BELT SANDING OF WOOD

Bolesław Porankiewicz,[a]* Adrián Banski,[b] and Grzegorz Wieloch [c]

This paper examines and discusses the specific belt sanding resistance K ($N \cdot cm^{-2}$) and specific belt sanding intensity SI ($g \cdot cm^{-2} \cdot min^{-1}$), for wood of *Pinus sylvestris* L., *Picea abies* L., *Quercus robra* L., *Acer pseudoplatanus* L., *Alnus glutinosa* Gaertn., *and Populus Nigra* L., by different sanding pressure p_S, different sanding grit N_G number, and different wood grain angles φ_v.

Keywords: Belt sanding; Specific sanding resistance; Specific sanding intensity; Sanding pressure; Sanding grit; Pinus sylvestris; Picea abies; Quercus robra; Acer pseudoplatanus; Alnus glutinosa; Populus nigra; Statistical dependencies

*Contact information: a: University of Zielona Góra, Szafrana 4, 65 516 Zielona Góra; Technical University of Zvolen, Masaryka 24, 96-001 Zvolen, Slovakia; c: University of Life Science, Poznań, Wojska Polskiego 28, 60 637 Poznań, Poland; *Corresponding author: poranek@amu.edu.pl*

INTRODUCTION

A narrow belt, elastic sanding process in directions from parallel, up to transverse to the wood grains, was carried out in an effort to determine the most efficient way to achieve the desired sanding quality, in terms of minimizing energy consumption and achieving results in the shortest time and the least wear of a belt sanding tool. The work piece after sanding ought to have defined dimensions, smoothness of the surface, and ought not to have burning marks (Porankiewicz and Wieloch 2008) or any kind of discolorizations.

A lot of researchers have analyzed such topics related to the consumption of time and costs (Taylor et al. 1999), aiming at work piece surface quality, sanding intensity, and power requirements (Banský et al. 1999, 2000; Banský 2004; Barcik and Vacek 1999; Matsumoto and Murase 1999; Očkajova 2002; Pahlitzsch and Dziobek 1959; Pahlitzsch and Dziobek 1961). However, the problem of sanding intensity and power consumption has not been worked out completely because of the large variety of sanding parameters, especially very many wood species, necessary for automation of a finishing operation. It has to be mentioned that in order to achieve the best sanding efficiency, different sanding parameters have to be applied for different wood species.

The present study attempts to evaluate the statistical dependencies of the narrow belt sanding specific resistance K ($N \cdot cm^{-2}$) and specific sanding intensity SI ($g \cdot cm^{-2} \cdot min^{-1}$) upon the most important machining parameters, including mechanical properties of six different European wood species examined.

EXPERIMENTAL

Experiments were done on a belt sanding laboratory stand (Fig. 1, Fig. 2) based on a portable Bosch GBS 100 AE belt sander, equipped in 6 step rotational speeds, and, Roventa individual vacuum cleaner, equipped with a paper filter bag, at the Technical University of Zvolen, Slovakia, under the following sanding conditions (where the values in brackets "< >" shows the minimum and maximum values of independent variables, and " .." marks show than many variables in a range were analyzed) :

1. Nominal power of electrical motor N_S=1.2 kW.
2. Active belt sanding wheel, rotational speed n_w=2613 min^{-1}.
3. Diameter of wheels of portable belt sanding machine d_w=57 mm.

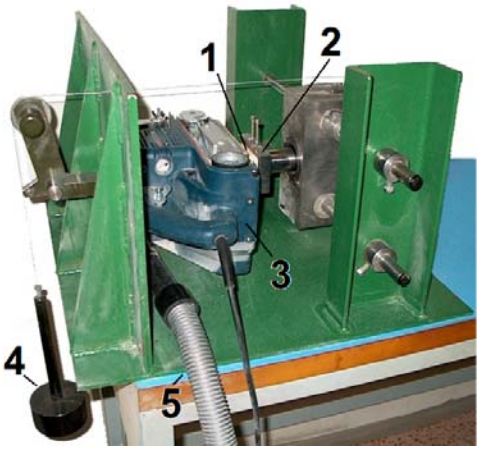

Fig. 1. Test stand; 1 - Wooden specimen, 2 - Wood specimen holder, 3 - Portable Bosch GBS 100 AE belt sander, 4 - Sanding load, 5 - Vacuum cleaner pipe

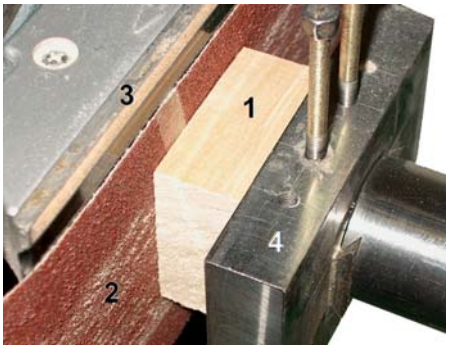

Fig. 2. Test stand; 1 - Wooden specimen, 2 - Sanding tool, 3 - Sanding foot, 4 - Wood specimen holder

4. Sanding belt circulation speed n_B=755 min^{-1}.
5. Sanding speed v_C=7.8 m/s.
6. Time of single sanding cycle t_S=1 min.
7. Elastic sanding load Q_S<25.56 .. 50.52> N.
8. Width of the sanding tool 100 mm.
9. Length of the belt sanding tool 620 mm.

10. Width, length and thickness of a wooden specimen 50 mm.
11. Area of the wooden specimen sanded A_S=25 cm^2.
12. Sanding pressure p_S<1.02 .. 2.01> N·cm^{-2}.
13. Number of grit of the electrocorunde sanding tool N_G: 35(*40); 15(*80); 10(*120); * - according to ANSI B 74, 18-1984.
14. Ranges of a grit size (according p. 15), in µm: 355-425; 150-180; 106-125.
15. Angle between sanding speed vector and wood grains φ_V=0; 60; 90°.
16. Angle between cutting plane and wood grains φ_S=0°.
17. Sanding process was conducted in tangential direction to wood grains.
18. Moisture content of the wooden specimen mc_{WP}=12 %.

Table 1. Properties of Wood Specimens Examined

	D kg·m^{-3}	R_T^*	R_S^*	R_C^* kG·cm^{-2}	R_B^*	$E\cdot10^{5*}$	C_R^{**} %
1 - *Pinus sylvestris* L.	551	1040	100	435	1000	1.2	3.65
2 - *Picea abies* L.	540	500	67	430	780	1.1	1.5
3 - *Quercus robra* L.	744	900	75	470	880	1.17	-
4 - *Acer pseudoplatanus* L.	619	820	90	490	950	0.94	-
5 - *Alnus glutinosa* Gaertn.	528	940	51	400	970	1.06	-
6 - *Populus nigra* L.	487	770	50	300	650	0.88	-

D - Wood density; R_T^* - Tensile strength radial; R_S^* - Share strength radial; R_C^* - Compression strength radial; R_B^* - Bending strength; E^* - Elasticity module.
Values marked by '*' were picked from work Wagenfür and Scheiber (1974) as overage ones by moisture content of mc_{WP}=12 %. Values marked by '**' were picked from work Lindgren and Norin (1969) as overage ones.

Wood specimens for experiments originated from Kováčová province of Slovakia, Europe. Primary breakdown was done at sawmill Bučina, Zvolen, Slovakia.
19. Wood density D<487 .. 744>kg·m^{-3}.

Dependent (observed) variables were as follows:
20. Specific sanding resistance K<0.579 .. 2.082> N·cm^{-2}.
21. Specific sanding intensity SI, defined by formula (1) <0.105 .. 1.637> g·cm^{-2}·min^{-1}.

$$SI = w_S \cdot A_S^{-1} \cdot t^{-1} \qquad (\text{g·cm}^{-2}\text{·min}^{-1}) \qquad (1)$$

where the new terms are:

w_S - weight of the removed wood from specimen sanded (g),
A_S - area of the wood specimens' surface sanded (mm^2),
t_S - time of sanding process (min),

22. Sanding feed speed, defined by formula (2) v_F<0.191 .. 2.35> mm·min^{-1}.

$$v_F = 10^4 \cdot SI \cdot D^{-1} \qquad (\text{mm·min}^{-1}) \qquad (2)$$

where the new term is:

D - wood density (kg·m^{-3}).

For evaluation of wood specimen's weight w_S (g) before and after sanding, a balance with accuracy 0.1 g was used. The specific sanding intensity SI (g·cm^{-2}·min^{-1}) was evaluated using formula (1). A specimen's dimensions before and after sanding were measured with use of a slice caliper with accuracy 0.02 mm.

A Corundum, endless belt sanding tool LS 308 XH was manufactured by Kilngspor. Sanding grit was attached to cotton fabric with use of resin. The opposite side of the sanding belt was impregnated by Teflon. Before use, the sanding tool and wood specimens were conditioned for 24 h in air having a relatively humidity as high as 65% and temperature as high as 20°C.

Active sanding power was measured with use of wattmeter MTP102, manufactured by Metra Blansko, Slovakia. The measuring signal was stored in an PC memory via an A/D converter. Belt sanding specific resistance K was evaluated from formula (3),

$$K = (P_S - P_I - P_T) \cdot v_C^{-1} \cdot t_S^{-1} \qquad (\mathrm{N \cdot cm^{-2}}) \qquad (3)$$

where the new terms are:

P_S - Active power of belt sanding (W)

P_I - Active power on idling (W)

P_F - Active power of friction of a sanding belt on a pressure foot (W).

Active power by idling P_I (W) was measured without the sanding belt. For measuring active power of friction of a sanding belt P_F (W) moving on a sanding foot, by sanding load Q_S (N) used, a special belt was prepared having a Teflon coating on both sides.

A statistical formula, of relations: $K=f(p_S, N_G, \varphi_V, D, R_T, R_S, R_C, R_B, E)$ (N·cm^{-2}) and $SI=f(p_S, N_G, \varphi_V, D, R_T, R_S, R_C, R_B, E)$ and $v_F=f(p_S, N_G, \varphi_V, D, R_T, R_S, R_C, R_B, E)$, should fit experimental matrix by the lowest summation of residuals square S_K, by the lowest standard deviation S_D, and by the highest correlation coefficient R between predicted and observed values. The formula also ought to have the proper influence of independent variables analyzed. A use of a simpler formula may result in decreasing approximation quality (larger S_K and S_D, and lower R), also a reverse impact of some independent variables may occur. It has to be reminded that a statistical relationship is valid only for ranges of independent variables defined in the experimental matrix; otherwise, for points lying outside the analyzed range of independent variables, significant error may take place. The fit quality of the statistical formula seems to be most important criterion of a choice, and discussion about that seems to be valuable in case of presence several studies performed under exactly the same machining conditions. In the evaluation process of statistical dependencies $K=f(p_S, N_G, \varphi_V, D, R_T, R_S, R_C, R_B, E)$ (N·cm^{-2}) and $SI=f(p_S, N_G, \varphi_V, D, R_T, R_S, R_C, R_B, E)$ (g·cm^{-2}·min^{-1}), and $v_f=f(p_S, N_G, \varphi_V, D, R_T, R_S, R_C, R_B, E)$ (mm·min^{-1}), linear functions, second order multinomial formulas, as well as power type and exponential functions without and with interactions were analyzed in preliminary calculations. According to assumptions discussed earlier in this study, the most adequate formulas appeared to be the equations (4)-(9).

$$K = a_1 + a_3 \cdot N_G + (a_4 \cdot \varphi_V^2 + a_5 \cdot \varphi_V) + a_6 \cdot D + a_7 \cdot R_T + a_8 \cdot R_S + a_9 \cdot R_C + a_{10} \cdot R_B + a_{11} \cdot E + MK$$
$$0.617 < K \pm S_D < 1.867 \text{ N·cm}^{-2} \quad (4)$$

$$MK = p_S \cdot [a_2 + a_{12} \cdot N_G + a_{13} \cdot R_B + a_{14} \cdot (a_{15} \cdot \varphi_V^2 + \mathrm{a}_{16} \cdot \varphi_V) + \mathrm{a}_{17} \cdot D + \mathrm{a}_{18} \cdot R_C + \mathrm{a}_{19} \cdot E] \quad (5)$$

$$SI = b_1 + b_3 \cdot N_G + (b_4 \cdot \varphi_V^2 + b_5 \cdot \varphi_V) + b_6 \cdot D + b_7 \cdot R_T + b_8 \cdot R_S + b_9 \cdot R_C + b_{10} \cdot R_B + b_{11} \cdot E + MS$$
$$0.114 < SI \pm S_D < 1.636 \text{ g·cm}^{-2}\text{·min}^{-1} \quad (6)$$

$$MS = p_S \cdot [b_2 + b_{12} \cdot N_G + b_{13} \cdot R_B + b_{14} \cdot (b_{15} \cdot \varphi_V^2 + \mathrm{b}_{16} \cdot \varphi_V) + \mathrm{b}_{17} \cdot D + \mathrm{b}_{18} \cdot R_C + \mathrm{b}_{19} \cdot E] \quad (7)$$

$$v_F = c_1 + c_3 \cdot N_G + (c_4 \cdot \varphi_V^2 + c_5 \cdot \varphi_V) + c_6 \cdot D + c_7 \cdot R_T + c_8 \cdot R_S + c_9 \cdot R_C + c_{10} \cdot R_B + c_{11} \cdot E + MV$$
$$0.191 < v_F \pm S_D < 2.35 \text{ mm·min}^{-1} \quad (8)$$

$$MV = p_S \cdot [c_2 + c_{12} \cdot N_G + c_{13} \cdot R_B + c_{14} \cdot (c_{15} \cdot \varphi_V^2 + \mathrm{c}_{16} \cdot \varphi_V) + \mathrm{c}_{17} \cdot D + \mathrm{c}_{18} \cdot R_C + \mathrm{c}_{19} \cdot E] \quad (9)$$

It has to be mentioned that 3 levels of independent variables variation was too low to properly fit a non-linear statistical formula, especially in case of expected presence of an extrema. Estimators for formula (4)-(5) were evaluated from an experimental matrix containing 214 measuring points (Table 2) and 178 measuring points for formula (6)-(7) and (8)-(9) (Table 3). There were done three repetition of each test. Each measuring point of both experimental matrixes was a average value from 3 replications. The necessary number of iterations for formulas (4)-(9) reached $1.5 \cdot 10^{10}$. During the evaluation process of formulas (4)-(9), elimination of unimportant or low important estimators was done by use of a coefficient of relatively importance C_{RI}, defined by formula (10), by assumption $C_{RI} > 0.1$.

$$C_{RI} = \left(S_k - S_{k0}\right) \cdot S_k^{-1} \cdot 100 \quad (\%) \quad (10)$$

In formula (10) the new terms are:

S_{K0k} - Summation of square of residuals, by c_k=0.

c_k - estimator with number k in statistical model evaluated.

Estimators assigned to the content of natural resin C_R (Table 1), having coefficient of relatively importance C_{RI} much lower value then limit, were excluded from formulas (4)-(9). The summation of residuals square S_K, a standard deviation S_D, a square of correlation coefficient of the predicted, and observed values R^2 were used for characterization of approximation quality. Calculations were performed at Poznań Networking & Supercomputing Center PCSS on an SGI Altix 3700 computer, using a special optimization program, based on a least squares method combined with gradient and Monte Carlo methods (Porankiewicz 1988) containing several later modifications.

RESULTS AND DISCUSSION

The following estimators for formula (4)-(5) describing the specific sanding resistance dependence $K=f(p_S, N_G, \varphi_V, D, R_T, R_S, R_C, R_B, E)$ (N·cm^{-2}): a_1=3.19259; a_2=-1.57317, a_3=3.82·10^{-3}, a_4=-0.47005, a_5=0.75813, a_6=-1.49·10^{-4}, a_7=-1.029·10^{-3}, a_8=1.181·10^{-3}, a_9=-6.838·10^{-3}, a_{10}=1.583·10^{-3}, a_{11}=-8.034·10^{-6}, a_{12}=-5.439·10^{-4}, a_{13}=-1.532·10^{-3}, a_{14}=250.525, a_{15}=-1.058·10^{-3}, a_{16}=1.683·10^{-3}, a_{17}=5.136·10^{-4}, a_{18}=3.88·10^{-3}, a_{19}=8.35·10^{-6} were evaluated. The approximation quality of fit of the formula (4)-(5) can be characterized by the quantifiers: S_K=5.34; R=0.87; R^2=0.75; S_D=0.16 N·cm^{-2} and also is illustrated in Fig. 3. The coefficients of relatively importance C_{RI} for estimators of formula (2)-(3) were as follows: C_{RI1}=40850, C_{RI2}=25890, C_{RI3}=436, C_{RI4}=2142, C_{RI5}=2724, C_{RI6}=29, C_{RI7}=3418, C_{RI8}=31, C_{RI9}=33878, C_{RI10}=7759, C_{RI11}=2924, C_{RI12}=2388, C_{RI13}=183, C_{RI14}=79, C_{RI15}=1775, C_{RI16}=2193, C_{RI17}=901, C_{RI18}=28465, C_{RI19}=8235. Figure 3 shows that the predicted specific sanding resistance K^P (N·cm^{-2}) was not perfectly correlated with the K (N·cm^{-2}) values observed. The largest variation as high as 0.75 N·cm^{-2} can be observed in the central part of the plot, while for the lowest values of the specific sanding resistance K^P (N·cm^{-2}) the variation was smaller. The reason for that may be the missing of an independent variable in the experimental matrix as well as inaccuracies of the specific sanding resistance K (N·cm^{-2}) measuring method. In the authors' opinion, the plot of predicted versus observed data points (Fig. 4) gives valuable, detailed, graphical information about approximation quality of evaluated statistical models.

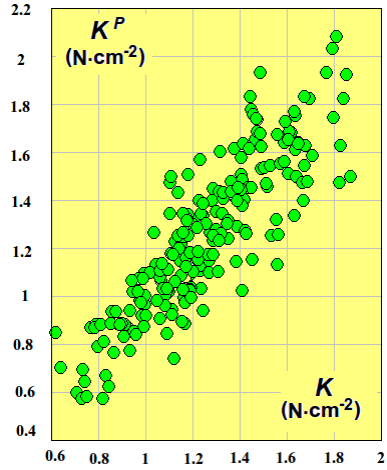

Fig. 3. The plot of specific sanding resistance K (N·cm^{-2}) observed, against predicted K^P (N·cm^{-2}) according to formula (4)-(5)

The use of average properties of wood species R_T (kG·cm^{-2}), R_S (kG·cm^{-2}), R_C (kG·cm^{-2}), R_B (kG·cm^{-2}), and E (kG·cm^{-2}), picked up from literature (Wagenfür and Scheiber 1974), as well as the D (kg·m^{-3}) allowed for successful evaluation of complete statistical dependencies $K=f(p_S, N_G, \varphi_V)$ (N·cm^{-2}) and $SI=f(p_S, N_G, \varphi_V)$ (g·cm^{-2}·min^{-1}) and $v_F=f(p_S, N_G, \varphi_V)$ (mm·min^{-1}) for all examined wood species; however, the representation of variation of D, R_T, R_S, R_C, R_B, and E independent variables was assigned to particular

wood species analyzed, literature average properties only. From this reason the relations $K=f(D, R_T, R_S, R_C, R_B, E)$ (N·cm^{-2}) and $SI=f(D, R_T, R_S, R_C, R_B, E)$ (g·cm^{-2}·min^{-1}) and $v_F=f(D, R_T, R_S, R_C, R_B, E)$ (mm·min^{-1}) cannot be extended to the whole range of their variation, where they might have limited merit or meaning. The wood properties (D, R_T, R_S, R_C, R_B and E) together with their estimators (a_7, a_8, a_9, a_{10}, a_{11}, a_{12}, a_{17}, a_{18}, a_{19}, a_{20}) and (b_6, b_7, b_8, b_9, b_{10}, b_{11}, b_{12}, b_{13}, b_{14}) and (c_6, c_7, c_8, c_9, c_{10}, c_{11}, c_{12}, c_{13}, c_{14}) have to be considered as constants for particular wood species for calculating specific sanding resistance K (N·cm^{-2}), specific sanding intensity SI (g·cm^{-2}·min^{-1}), and average, elastic feed speed dependency v_F (mm·min^{-1}). In future work it is recommended to take into account real values of the wood specimens physical and mechanical properties used in experiment, as well as a wider range of variation of every wood species.

The Influence of Sanding Parameters on the Specific Sanding Resistance *K*

$$K^{PS}=0.59496+3.82\cdot10^{-3}\cdot N_G+(-0.47005\cdot\varphi_V^2+0.75813\cdot\varphi_V)+MK^{PS} \text{ (N·cm}^{-2}\text{)} \quad (11)$$

$$MK^{PS}=p_S\cdot[0.85569-1.532\cdot10^{-3}\cdot N_G-250.525\cdot(1.058\cdot10^{-3}\cdot\varphi_V^2+1.683\cdot10^{-3}\cdot\varphi_V)] \quad (12)$$

For wood of the ***Pinus sylvestris* L.**, after substituting constants D, R_T, R_S, R_C, R_B, and E, the formula (4)-(5) took the form of (11)-(12), which is represented by the plot in Fig. 4, showing t hat the specific sanding resistance K (N·cm^{-2}) significantly depended

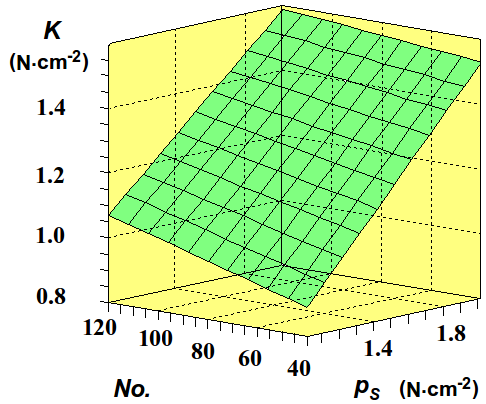

Fig. 4. Dependence between the specific sanding resistance K (N·cm^{-2}) and the sanding pressure p_S (N·cm^{-2}), and the number of sanding grit N_O, according to formula (11)-(12); sanding parameters: φ_V=60°, D=551 kg·m^{-3}, R_T=1040 kG·cm^{-2}, R_S=100 kG·cm^{-2}, R_C=435 kG·cm^{-2}, R_B=1000 kG·cm^{-2}, E=120·10^3 kG·cm^{-2} (*Pinus sylvestris* L.)

upon the sanding pressure p_S (N·cm^{-2}). An increase of the sanding pressure strongly enlarges the specific sanding resistance K (N·cm^{-2}). The influence of grit number N_G on the specific sanding resistance K (N·cm^{-2}) was lower than sanding pressure p_S (N·cm^{-2}), by a linear tendency. With grit number N_G increasing, and also with a mean decrease of the sanding grit size, the specific sanding resistance K (N·cm^{-2}) was enlarged. This was due to an increase of active sanding grits number at the same time, as well as decrease of a cheap thickness. This influence dropped down with sanding pressure increase up to

p_S=2.02 N·cm^{-2}. The general shape of relations $K=f(p_S, N_G)$ (N·cm^{-2}) shown in Figs. 6 up to 9 were similar for all of wood specimens analyzed.

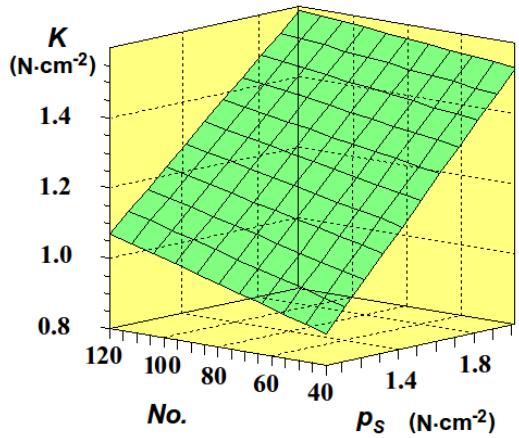

Fig. 5. Dependence between the specific sanding resistance K (N·cm^{-2}) and the sanding pressure p_S (N·cm^{-2}), and the number of sanding grit N_O, according to formula (13)-(14); sanding parameters: φ_V=60°, D=540 kg·m^{-3}, R_T=500 kG·cm^{-2}, R_S=67 kG·cm^{-2}, R_C=430 kG·cm^{-2}, R_B=780 kG·cm^{-2}, E=110·10^3 kG·cm^{-2} (*Picea abies* L.)

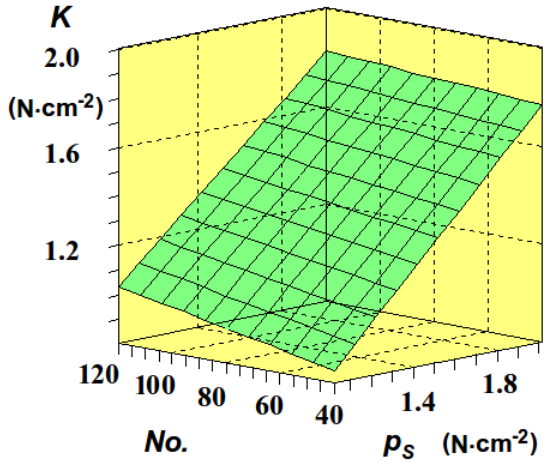

Fig. 6. Dependence between the specific sanding resistance K (N·cm^{-2}) and the sanding pressure p_S (N·cm^{-2}), and the number of sanding grit N_O, according to formula (15)-(16); sanding parameters: φ_V=60°, D=744 kg·m^{-3}, R_T=900 kG·cm^{-2}, R_S=75 kG·cm^{-2}, R_C=470 kG·cm^{-2}, R_B=880 kG·cm^{-2}, E=117·10^3 kG·cm^{-2} (*Quercus robra* L.)

$$K^{PA}=0.08748+3.82\cdot10^{-3}\cdot N_G+(-0.47005\cdot\varphi_V^2+0.75813\cdot\varphi_V)+MK^{PA}\ \text{(N·cm-2)} \quad (13)$$

$$MK^{PA}=p_S\cdot[0.74714-1.532\cdot10^{-3}\cdot N_G-250.525\cdot(1.058\cdot10^{-3}\cdot\varphi_V^2+1.683\cdot10^{-3}\cdot\varphi_V)] \quad (14)$$

For wood of ***Picea abies*** **L.**, after substituting constants D, R_T, R_S, R_C, R_B, and E, the formula (4)-(5) took the form of (13)-(14), the plot of which is shown in Fig. 5. The maximum and minimum values of the K (N·cm^{-2}), as large as K=0.74 N·cm^{-2} and K=1.41 N·cm^{-2}, were smaller in comparison to wood of *Pinus sylvestris* L., by as much as 17 %

and 11 % respectively, which follows from the fact that the average mechanical properties of wood of *Picea abies* L., in comparison to *Pinus sylvestris* L. wood, were dictated by very similar contents of cellulose and lignin.

$$K^{Q}=-0.51643+3.82\cdot10^{-3}\cdot N_G+(-0.47005\cdot\varphi_V^2+0.75813\cdot\varphi_V)+MK^{Q}\ (\mathrm{N\cdot cm^{-2}}) \quad (15)$$

$$MK^{Q}=p_S\cdot[1.13082-1.532\cdot10^{-3}\cdot N_G-250.525\cdot(1.058\cdot10^{-3}\cdot\varphi_V^2+1.683\cdot10^{-3}\cdot\varphi_V)] \quad (16)$$

For wood of the ***Quercus robra* L.**, after substituting of constants D, R_T, R_S, R_C, R_B, and E, the formula (4)-(5) took the form of equation (15)-(16), which plot is shown in Fig. 6. The minimum value of the K ($\mathrm{N\cdot cm^{-2}}$) for wood of *Quercus robra* L., as large as K=0.85 $\mathrm{N\cdot cm^{-2}}$, was 1% lower that one for *Pinus sylvestris* L. wood. This observation might be attributed to lower content of cellulose (42.8 %) and higher content of lignin (34.3 %) (Wagenfür and Scheiber 1974) in chemical composition of *Quercus robra* L. wood, known as friction coefficient decreasing factors. At the same time the maximum, observed by the highest sanding pressure p_S ($\mathrm{N\cdot cm^{-2}}$), as large as K=1.83 $\mathrm{N\cdot cm^{-2}}$, was as much as 13 % larger than that of *Pinus sylvestris* L. wood, which follows from a higher density D ($\mathrm{kg\cdot m^{-3}}$) and compression strength R_C ($\mathrm{kG\cdot cm^{-2}}$) of the *Quercus robra* L. specimen.

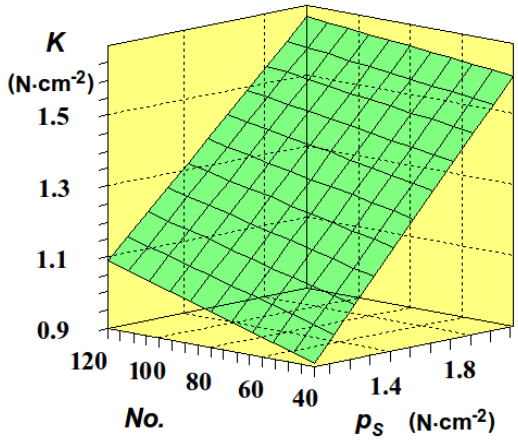

Fig. 7. Dependence between the specific sanding resistance K ($\mathrm{N\cdot cm^{-2}}$) and the sanding pressure p_S, and the number of sanding grit N_O, according to formula (17)-(18); sanding parameters: φ_V=60°, D=619 $\mathrm{kg\cdot m^{-3}}$, R_T=820 $\mathrm{kG\cdot cm^{-2}}$, R_S=90 $\mathrm{kG\cdot cm^{-2}}$, R_C=490 $\mathrm{kG\cdot cm^{-2}}$, R_B=950 $\mathrm{kG\cdot cm^{-2}}$, E=$94\cdot10^3$ $\mathrm{kG\cdot cm^{-2}}$ (*Acer pseudoplatanus* L.)

For wood of the ***Acer pseudoplatanus L.*** after substituting constants D, R_T, R_S, R_C, R_B, and E, the formula (4)-(5) took the form of (17)-(18), for which the corresponding plot was shown in Fig. 7. The minimum and maximum values for this wood specimen, as high as K=0.91 $\mathrm{N\cdot cm^{-2}}$ and K=1.67 $\mathrm{N\cdot cm^{-2}}$, were larger by as much as 2% and 6%, respectively, in comparison to *Pinus sylvestris* L. wood, following higher wood density D ($\mathrm{kg\cdot m^{-3}}$) and compression strength R_C ($\mathrm{kG\cdot cm^{-2}}$) of wood of *Acer pseudoplatanus* L. in comparison to *Pinus sylvestris* L. wood, which also was in agreement for wood of *Quercus robra* L. for the maximum value shown in Fig. 8. However it cannot be

explained why the minimum value of the K=0.91 N·cm^{-2} for wood of *Acer pseudoplatanus* L. was larger than for wood of *Quercus robra L.*

$$K^{AP}=-0.23898+3.82\cdot10^{-3}\cdot N_G+(-0.47005\cdot\varphi_V^2+0.75813\cdot\varphi_V)+MK^{AP}\ (\mathrm{N\cdot cm^{-2}}) \quad (17)$$

$$MK^{AP}=p_S\cdot[0.65379-1.532\cdot10^{-3}\cdot N_G-250.525\cdot(1.058\cdot10^{-3}\cdot\varphi_V^2+1.683\cdot10^{-3}\cdot\varphi_V)] \quad (18)$$

For wood of the ***Alnus glutinosa* Gaertn.** after substituting constants D, R_T, R_S, R_C, R_B, and E into the formula (4)-(5) took the form of (19)-(20), the plot for which is shown in Fig. 8. The minimum value for this wood specimen, as high as K=0.99 N·cm^{-2} was 11% larger, in comparison to *Pinus sylvestris* L. wood, which was not in agreement with D, R_T, R_S, R_C, R_B, and E properties. The maximum value for wood of *Alnus glutinosa* Gaertn., as high as K=1.44 N·cm^{-2}, was 9% smaller in comparison to *Pinus sylvestris* L. wood., and also smaller for wood of *Acer pseudoplatanus* L. and *Quercus robra* L., following D, R_T, R_S, R_C, R_B, and E properties.

$$K^{AG}=0.15572+3.82\cdot10^{-3}\cdot N_G+(-0.47005\cdot\varphi_V^2+0.75813\cdot\varphi_V)+MK^{AG}\ (\mathrm{N\cdot cm^{-2}}) \quad (19)$$

$$MK^{AG}=p_S\cdot[0.6075-1.532\cdot10^{-3}\cdot N_G-250.525\cdot(1.058\cdot10^{-3}\cdot\varphi_V^2+1.683\cdot10^{-3}\cdot\varphi_V)] \quad (20)$$

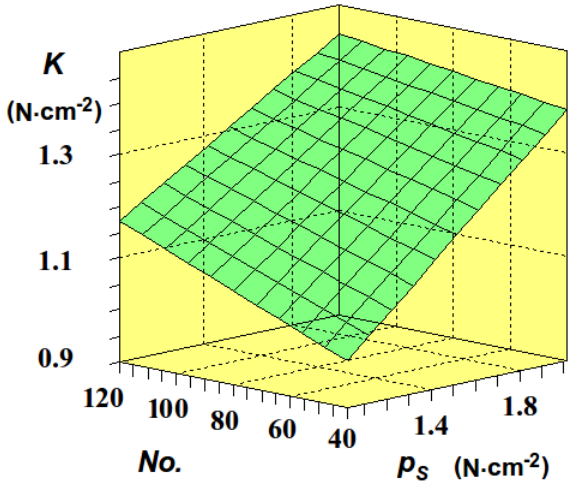

Fig. 8. Dependence between the specific sanding resistance K (N·cm^{-2}) and the sanding pressure p_S, and the number of sanding grit N_O, according to formula (19)-(20); sanding parameters: φ_V=60°, D=528 kg·m^{-3}, R_T=940 kG·cm^{-2}, R_S=51 kG·cm^{-2}, R_C=400 kG·cm^{-2}, R_B=970 kG·cm^{-2}, E=106·10^3 kG·cm^{-2} (*Alnus glutinosa* Gaertn.)

For wood of the ***Populus nigra* L.** after substituting constants D, R_T, R_S, R_C, R_B, and E, the formula (4)-(5) took the form of (21)-(22), which is plotted in Fig. 9, showing that the general shape of relation $K=f(p_S)$ (N·cm^{-2}) for number of grit N_o>40, was opposite to that obtained for *Pinus sylvestris* L. An increase of sanding pressure from p_S=1.02 N·cm^{-2} to p_S=2.02 N·cm^{-2}, decreased as much as 9% the specific sanding resistance from the value K=1.28 N·cm^{-2} to the value K=1.17 N·cm^{-2}. This phenomenon cannot be explained on the ground of properties of wood specimens examined. The minimum value

of the K (N·cm^{-2}) for the wood of *Populus nigra* L., as high as K=1.1 N·cm$^{-2,}$ was as much as 19 % larger in comparison to *Pinus sylvestris* L. wood. This observation might be explained by the highest content of cellulose of 60% in wood of *Populus nigra* L., the largest of all analyzed wood species (Wagnefür and Scheiber 1974), and a low content of lignin, which are known as factors tending to increase the coefficient of friction.

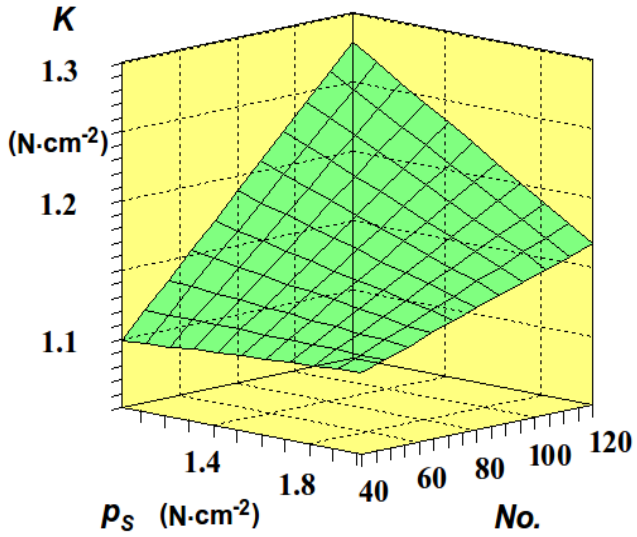

Fig. 9. Dependence between the specific sanding resistance K (N·cm^{-2}) and the sanding pressure p_S (N·cm^{-2}) and the number of sanding grit N_O, according to formula (21)-(22); sanding parameters: φ_V=60°, D=487 kg·m^{-3}, R_T=770 kG·cm^{-2}, R_S=50 kG·cm^{-2}, R_C=300 kG·cm^{-2}, R_B=650 kG·cm^{-2}, E=88·10^3 kG·cm^{-2} (*Populus nigra* L.)

$$K^{PN} = 0.657428 + 3.82 \cdot 10^{-3} \cdot N_G + (-0.47005 \cdot \varphi_V^2 + 0.75813 \cdot \varphi_V) + MK^P \text{ (N·cm}^{-2}\text{)} \quad (21)$$

$$MK^{PN} = p_S \cdot [0.2222 - 1.532 \cdot 10^{-3} \cdot N_G - 250.525 \cdot (1.058 \cdot 10^{-3} \cdot \varphi_V^2 + 1.683 \cdot 10^{-3} \cdot \varphi_V)] \quad (22)$$

The impact of the sanding pressure p_S (N·cm^{-2}) on the specific belt sanding resistance K (N·cm-2), only in case of it's largest values, followed the average density D (kg·m^{-3}) and the compression strength R_C (kG·cm^{-2}), in the case of *Pinus sylvestris* L., *Picea abies* L., *Quercus robra* L., *Acer pseudoplatanus* L. The specific sanding resistance K (N·cm^{-2}) was larger for sanding with use of sanding grit number N_G=120, for examined wood species (Fig. 4 up to Fig. 9), with the exception of the wood of *Populus nigra* L. Figures 5 to 10 show that the specific sanding resistance K (N·cm^{-2}) was the smallest for sanding with use of sanding grit number N_G=40, for all examined wood species.

The impact of the wood grain angle φ_V(°), and the sanding pressure p_S (N·cm^{-2}) on the specific sanding resistance K (N·cm^{-2}), was very complex for all wood specimens examined. The general shape of relation $K=f(p_S, \varphi_V)$ (N·cm^{-2}) is shown in Fig. 10 up to Fig. 15 for all wood specimens analyzed was similar.

The plot of relation for wood of ***Pinus sylvestris* L.**, according to formulas (11)-(12) is shown in Fig. 10, where two minima, as small as K=0.77 N·cm^{-2} and K=0.79

N·cm^{-2}, at angles φ_V=0° and φ_V=90°, and one maximum as high as K=0.9 N·cm^{-2}, at angle φ_V=40°, for the lowest sanding pressure p_S=1.02 N·cm^{-2}, as well as one minimum, as small as K=1.53 (N·cm^{-2}), at angle φ_V=47°, and two maxima, as high as K=1.56 (N·cm^{-2}) and K=1.57 (N·cm^{-2}), at angles φ_V=0° and φ_V=90°, for the largest sanding pressure p_S=2.02 N·cm^{-2} can be seen. At the sanding pressure p_S=1.82 N·cm^{-2}, minima and maxima disappeared. The angle positions of minima and maxima remained unchanged for all wood species examined. The reason of such a complex impact of the the wood grain angle φ_V (°) and sanding pressure p_S (N·cm^{-2}) on the specific sanding resistance K (N·cm^{-2}) might be a different chip formation in the space between sanding grits; however more experiments are needed to explain this phenomenon.

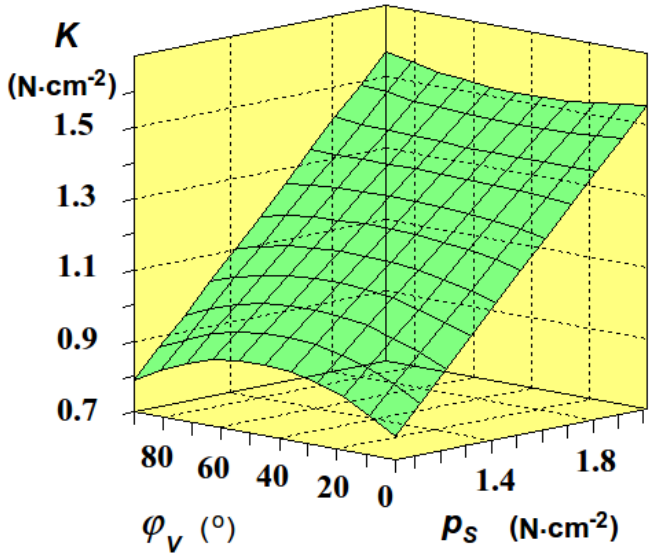

Fig. 10. The impact between wood grains angle φ_V (°), and the sanding pressure p_S (N·cm^{-2}) on the specific sanding resistance K (N·cm^{-2}), according to formula (11)-(12); sanding parameters: N_G=40, D=551 kg·m^{-3}, R_T=1040 kG·cm^{-2}, R_S=100 kG·cm^{-2}, R_C=435 kG·cm^{-2}, R_B=1000 kG·cm^{-2}, E=120·10^3 kG·cm^{-2} (*Pinus sylvestris* L.)

For wood of the ***Picea abies* L.**, the plot according to formula of (13)-(14) set in Fig. 11, showed that for the lowest sanding pressure p_S=1.02 N·cm^{-2}, two minima, and one maximum were smaller by 19%, 19%, and 17%, respectively, than one for wood of for *Pinus sylvestris* L. For the largest sanding pressure of p_S=2.02 N·cm^{-2}, two maxima, and one minimum were 12 % smaller than one for wood of for *Pinus sylvestris* L.

For wood of ***Quercus robra* L.**, plotted in Fig. 12, results according to formula (15)-(16) showed that for the lowest sanding pressure p_S=1.02 N·cm^{-2}, two minima and one maximum were smaller by 5%, 5%, and 4%, respectively, than one for wood of *Pinus sylvestris* L. For the largest sanding pressure of p_S=2.02 N·cm^{-2}, two maxima and one minimum were larger by 13%, 13%, and 8%, respectively, than that for the wood of *Pinus sylvestris* L.

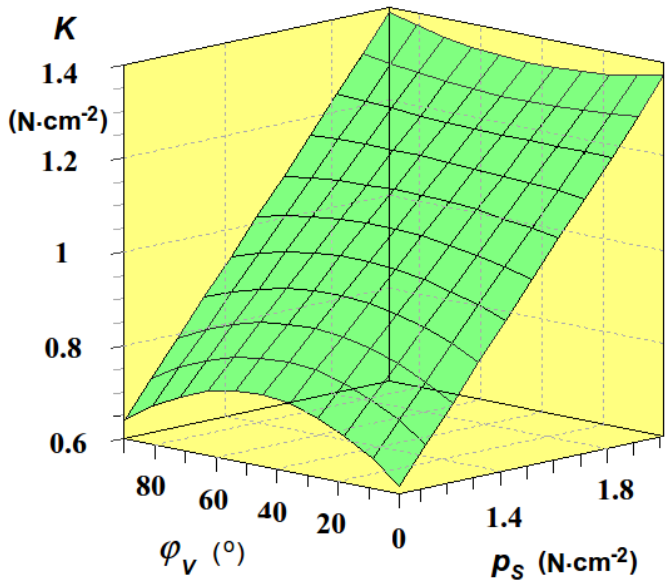

Fig. 11. The impact of the wood grain angle φ_V (°), and the sanding pressure p_S (N·cm^{-2}) on the specific sanding resistance K (N·cm^{-2}), according to formula (13)-(14); sanding parameters: N_G=40, D=540 kg·m^{-3}, R_T=500 kG·cm^{-2}, R_S=67 kG·cm^{-2}, R_C=430 kG·cm^{-2}, R_B=780 kG·cm^{-2}, E=110·10^3 kG·cm^{-2} (*Picea abies* L.)

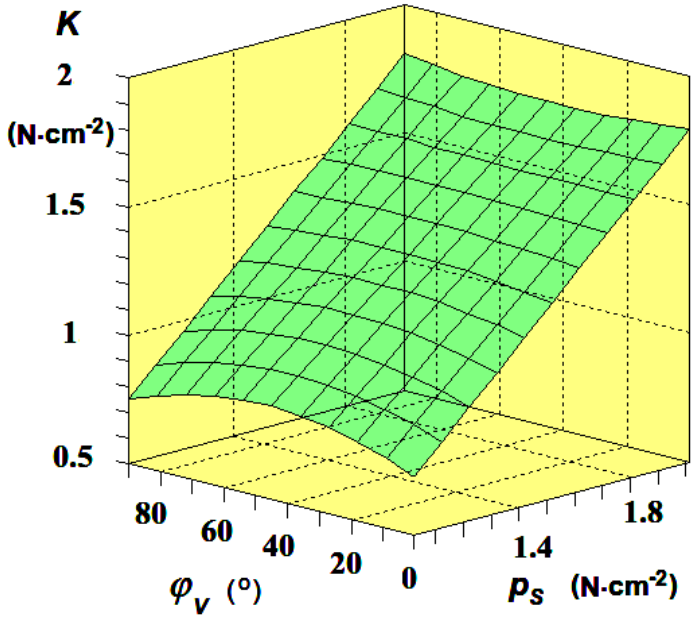

Fig. 12. The impact of the wood grain angle φ_V (°), and the sanding pressure p_S (N·cm^{-2}) on the specific sanding resistance K (N·cm^{-2}), according to formula (15)-(16); sanding parameters: N_G=40, D=744 kg·m^{-3}, R_T=900 kG·cm^{-2}, R_S=75 kG·cm^{-2}, R_C=470 kG·cm^{-2}, R_B=880 kG·cm^{-2}, E=117·10^3 kG·cm^{-2} (*Quercus robra* L.)

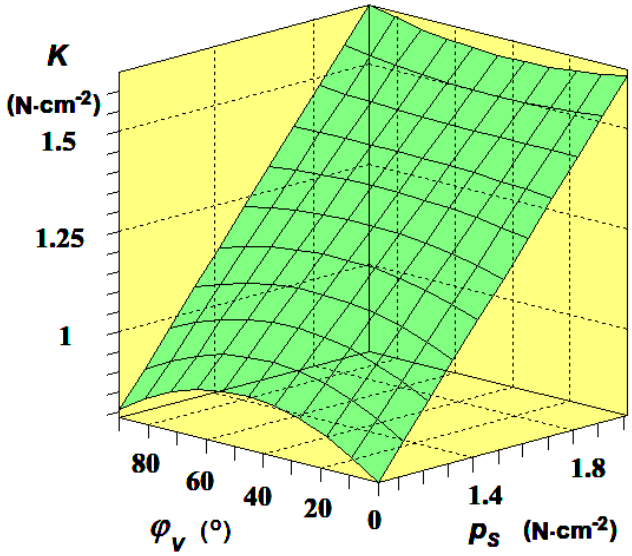

Fig. 13. The impact of the wood grain angle φ_V (°) and the sanding pressure p_S (N·cm^{-2}) on the specific sanding resistance K (N·cm^{-2}), according to formula (17)-(18); sanding parameters: N_G=40, D=619 kg·m^{-3}, R_T=820 kG·cm^{-2}, R_S=90 kG·cm^{-2}, R_C=490 kG·cm^{-2}, R_B=950 kG·cm^{-2}, E= 94·10^3 kG·cm^{-2} (*Acer pseudoplatanus* L.)

For wood of ***Acer pseudoplatanus* L.**, the plot in Fig. 13 according to formula (17)-(18) showed that the for the lowest sanding pressure p_S=1.02 N·cm^{-2}, two minima, and one maximum were larger by 1%, 2%, and 1%, respectively, than one for the wood of *Pinus sylvestris L*. For the largest sanding pressure of p_S=2.02 N·cm^{-2}, two maxima, and one minimum were larger by 4%, 5%, and 4%, respectively, than one for the wood of *Pinus sylvestris* L.

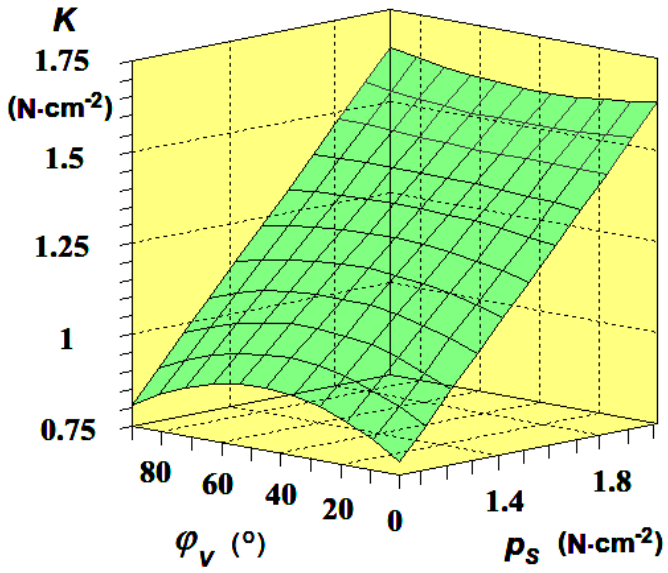

Fig. 14. The impact of the wood grain angle φ_V (°), and the sanding pressure p_S (N·cm^{-2}) on the specific sanding resistance K (N·cm^{-2}), according to formula (19)-(20); sanding parameters: N_G=40, D=528 kg·m^{-3}, R_T=940 kG·cm^{-2}, R_S=51 kG·cm^{-2}, R_C=400 kG·cm^{-2}, R_B=970 kG·cm^{-2}, E=106·10^3 kG·cm^{-2} (*Alnus glutinosa* Gaertn.)

The plot in the Fig. 14 for wood of ***Alnus glutinosa* Gaertn.**, according to formula (19)-(20) showed that for the lowest sanding pressure p_S=1.02 N·cm^{-2}, two minima, and one maximum were larger, by as much as 11%, 11%, and 10%, respectively than that of wood of for *Pinus sylvestris* L. For the largest sanding pressure of p_S=2.02 N·cm^{-2}, two maxima, and one minimum were smaller by 10%, 9%, and 10%, respectively ,than one for the wood of *Pinus sylvestris* L.

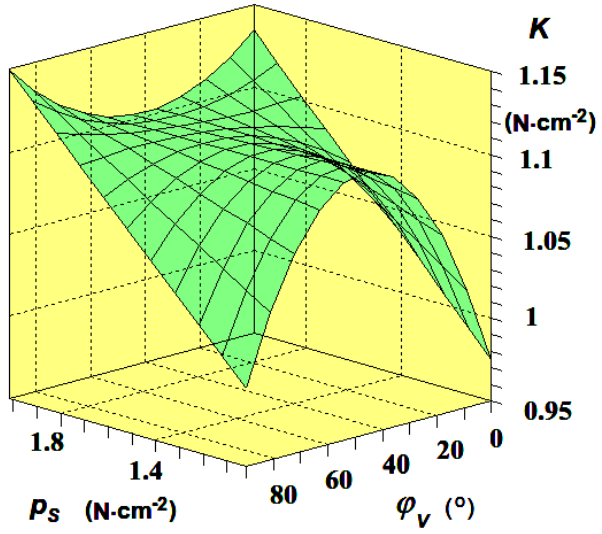

Fig. 15. The impact of the wood grain angle φ_V (°), and the sanding pressure p_S (N·cm^{-2}) on the specific sanding resistance K (N·cm^{-2}), according to formula (21)-(22); sanding parameters: N_G=40, D=487 kg·m^{-3}, R_T=770 kG·cm^{-2}, R_S=50 kG·cm^{-2}, R_C=300 kG·cm^{-2}, R_B=650 kG·cm^{-2}, E=88·10^3 kG·cm^{-2} (*Populus nigra* L.)

For the wood of the ***Populus nigra* L.**, according to formula of (21)-(22), the plot is shown in Fig. 16. For the lowest sanding pressure p_S=1.02 N·cm^{-2}, two minima, and one maximum were larger by as much as 15%, 21%, and 19%, respectively, than that for the wood of *Pinus sylvestris* L. The value of K (N·cm^{-2}) obtained for the lowest sanding pressure of p_S=1.02 N·cm^{-2}, was the largest of all wood specimens examined, in spite of the fact that all physical and mechanical properties of wood of *Populus nigra* L. were the lowest. The only reason to explain these findings might be that the largest of all examined wood species, the content of cellulose was 60% in the wood of *Populus nigra* L. (Wagnefür and Scheiber 1974), known as friction coefficient increase factor. However more experiments are needed to explain this phenomenon. For the largest sanding pressure of p_S=2.02 N·cm^{-2}, two minima, and one maximum were smaller, by as much as 28%, 27%, and 35%, respectively, than that of the wood of *Pinus sylvestris* L.

Figures 10 up to 15 show that the specific sanding resistance K (N·cm^{-2}) was larger for transversely sanding, by wood grain angle φ_V=90°, in comparison to sanding parallel to wood grains by angle φ_V=0°, for all the examined wood species. The largest maximum of K (N·cm^{-2}) observed for the largest sanding pressure p_S (N·cm^{-2}) and wood of *Quercus robra* L. might be related only to wood density D (kg·m^{-3}). This tendency was not observed for minimum values of the K (N·cm^{-2}), observed for the lowest sanding pressure p_S (N·cm^{-2}), for which the issue of influence of wood properties taken into

account on the belt sanding specific resistance K (N·cm^{-2}) seemed to be very complex. The experiments performed, however, were not sufficient for explanation of this phenomenon.

The Influence of Sanding Parameters on Specific Sanding Intensity *SI*

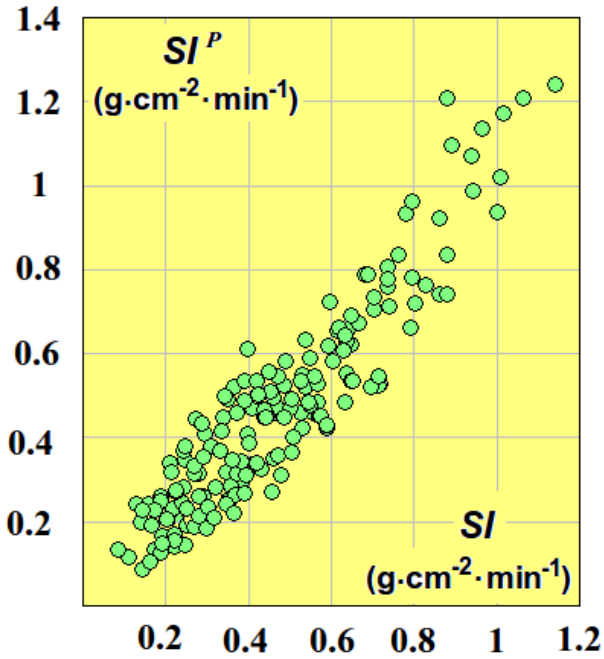

Fig. 16. Plot of the specific sanding intensity *SI* (g·cm^{-2}·min^{-1}) observed, against predicted SI^P (g·cm^{05}·min^{-1}), according to formula (6)-(7)

For formula (6)-(7), describing specific sanding intensity dependency $SI=f(p_S,N_G, \varphi_V, D, R_T, R_S, R_C, R_B, E)$ (g·cm-2·min-1), the following estimators were evaluated: b_1=1.83586, b$_2$=-0.55478, b_3=3.055·10^{-3}, b_4=0.06881, b_5=-0.03754, b_6=-1.426·10^{-4}, b_7=-1.546·10^{-3}, b_8=-2.379·10^{-3}, b_9=-8.082·10^{-5}, b_{10}=-4.596·10^{-5}, b_{11}=-4.72·10^{-6}, b_{12}=9.614·10^{-4}, b_{13}=9.706·10^{-6}, b_{14}=-0.4687, b_{15}=0.07063, b16=-0.09766, b_{17}=-3.682·10^{-3}, b_{18}=-4.368·10^{-6}, b_{19}=-1.564·10^{-3}. The quality of approximation of the fit of the formula (6)-(7) is shown in Fig. 17 and was also characterized by the quantifiers: S_K=1.56, R=0.92, R^2=0.85, S_D=0.09 g·cm^{-2}·min^{-1}. The coefficients of relative importance C_{RI} for estimators of formula (6)-(7) were as follows: C_{RI1}=38187, C_{RI2}=9077, C_{RI3}=792, C_{RI4}=60, C_{RI5}=36, C_{RI16}=79, C_{RI7}=23024, C_{RI8}=391, C_{RI9}=15, C_{RI10}=20, C_{RI11}=3035, C_{RI12}=22896, C_{RI13}=33271, C_{RI14}=39, C_{RI15}=36, C_{RI16}=145, C_{RI17}=2992, C_{RI18}=0.2, and C_{RI19}=14339. Figure 17 shows that the largest variation, as high as 0.31 g·cm^{-2}·min^{-1}, can be observed in the central part of the plot, while for the lowest and for the largest values of the sanding intensity SI^P (g·cm^{-2}·min^{-1}), the variation was much smaller. Some contribution of relatively large variation of results of specific sanding resistance K (N·cm^{-2}) and specific sanding intensity SI (g·cm^{-2}·min^{-1}) observed might have it's uncontrolled source in the dynamic properties of the measuring stand used.

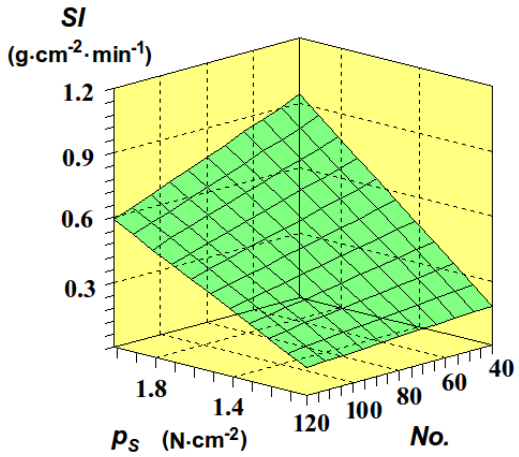

Fig. 17. Dependence between the specific sanding intensity *SI* (g·cm^{-2}·min^{-1}) and the sanding pressure p_S (N·cm^{-2}) and the number of sanding grit N_G, according to formula (23)-(24); sanding parameters: φ_V=60°, *D*=551 kg·m^{-3}, R_T=1040 kG·cm^{-2}, R_S=100kG·cm^{-2}, R_C=435 kG·cm^{-2}, R_B=1000 kG/cm^2, *E*=120·10^3 kG·cm^{-2} (*Pinus sylvestris* L.)

$$SI^{PS} = -0.738758 + 3.055 \cdot 10^{-3} \cdot N_G + (0.06881 \cdot \varphi_V^2 - 0.03754 \cdot \varphi_V) + Mk^{PS} \quad (23)$$

$$MS^{PS} = p_S \cdot [0.88862 - 9.614 \cdot 10^{-4} \cdot N_G - 0.4687 \cdot (0.07063 \cdot \varphi_V^2 - 0.09766 \cdot \varphi_V)] \quad (24)$$

The plot shown in Fig.17, according to formula (23)-(24), between sanding intensity *SI* (g·cm^{-2}·min^{-1}) and the sanding pressure p_S (N·cm^{-2}) and the sanding grit number N_G for ***Pinus sylvestris* L.** wood specimen, showed that the specific sanding intensity *SI* (g·cm^{-2}·min^{-1}) strongly depended upon the sanding pressure p_S (N·cm^{-2}). An increase of the sanding pressure strongly enlarges the sanding intensity *SI* (g·cm^{-2}·min^{-1}), more for the smallest grit number N_G and less for the largest grit number N_G. The influence of grit number N_G on the specific sanding intensity *SI* (g·cm^{-2}·min^{-1}) was lower then the sanding pressure p_S (N·cm^{-2}), having the same tendency. An increase of the grit

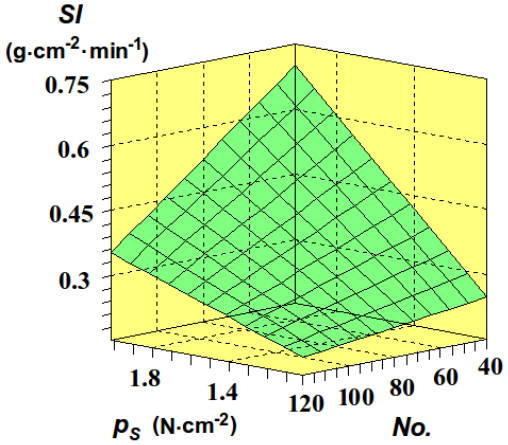

Fig. 18. The impact of the specific sanding intensity *SI* (g·cm^{-2}·min^{-1}) and the sanding pressure p_S (N·cm^{-2}) and the number of sanding grit N_G, according to formula (25)-(26); sanding parameters: φ_V=60°, *D*=540 kg·m^{-3}, R_T=500 kG·cm^{-2}, R_S=67 kG·cm^{-2}, R_C=430 kG·cm^{-2}, R_B=780 kG·cm^{-2}, *E*=110·10^3 kG·cm^{-2} (*Picea abies* L.)

number N_G dropped down the specific sanding intensity SI (g·cm^{-2}·min^{-1}), much more for the largest sanding pressure p_S (N·cm^{-2}) and less for the smallest sanding pressure p_S (N·cm^{-2}). The general shape of plots of this relation for all wood specimens examined, shown in Fig. 17 up to Fig. 21 was similar.

The plot of relation set in Fig.18, according to formula (25)-(26), for wood of *Picea abies* L., illustrated that the maximum value of the SI (g·cm^{-2}·min^{-1}), as high as SI=0.7 g·cm^{-2}·min^{-1} was 25% smaller in comparison to *Pinus sylvestris* L., while the minimum value of the SI (g·cm^{-2}·min^{-1}), as high as SI=0.25 g·cm^{-2}·min^{-1}, was 25% higher in comparison to the *Pinus sylvestris* L. wood specimen.

$$SI^{PA}=0.235273+3.055\cdot10^{-3}\cdot N_G+(0.06881\cdot\varphi_V^2-0.03754\cdot\varphi_V)+MS^{PA} \quad (25)$$

$$MS^{PA}=p_S\cdot[0.799433-9.614\cdot10^{-4}\cdot N_G-0.4687\cdot(0.07063\cdot\varphi_V^2-0.09766\cdot\varphi_V)] \quad (26)$$

The plot in Fig. 19, according to formula (27)-(28), for wood of ***Quercus robra* L.**, showed that the maximum value of the sanding intensity SI (g·cm^{-2}·min^{-1}), as high as SI=0.8 g·cm^{-2}·min^{-1} was smaller, by as much as 15% in comparison to *Pinus sylvestris* L., while the minimum value of the SI (g·cm^{-2}·min^{-1}), as high as SI=0.25 g·cm^{-2}·min^{-1} was higher, by as much as 25% in comparison to the *Pinus sylvestris L* wood specimen.

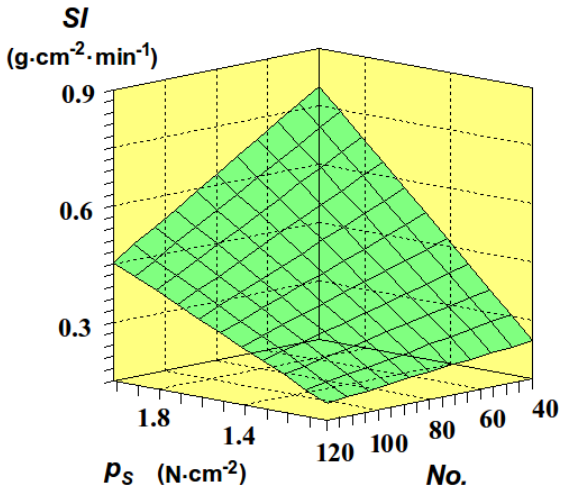

Fig. 19. The impact of the specific sanding intensity SI (g·cm^{-2}·min^{-1}) and the sanding pressure p_S (N·cm^{-2}) and the number of sanding grit N_G, according to formula (27)-(28); sanding parameters: φ_V=60°, D=744 kg·m^{-3}, R_T=900 kG·cm^{-2}, R_S=75 kG·cm^{-2}, R_C=470 kG·cm^{-2}, R_B=880 kG·cm^{-2}, E=117·10^3 kG·cm^{-2} (*Quercus robra* L.)

$$SI^{Q}=-0.473177+3.055\cdot10^{-3}\cdot N_G+(0.06881\cdot\varphi_V^2-0.03754\cdot\varphi_V)+MS^{Q} \quad (27)$$

$$MS^{Q}=p_S\cdot[0.688553-9.614\cdot10^{-4}\cdot N_G-0.4687\cdot(0.07063\cdot\varphi_V^2-0.09766\cdot\varphi_V)] \quad (28)$$

The plot in Fig. 20, according to formula (29)-(30), for wood of ***Acer pseudoplatanus* L.**, showed that the maximum value of the *SI* (g·cm^{-2}·min^{-1}), as high as *SI*=0.64 g·cm^{-2}·min^{-1} was, by as much as 32% smaller in comparison to *Pinus sylvestris* L., while the minimum value of the *SI* (g·cm^{-2}·min^{-1}), as high as *SI*=0.27 g·cm^{-2}·min^{-1} was higher, by as much as 30 % in comparison to the *Pinus sylvestris* L. wood specimen.

$$SI^{AP} = -0.263398 + 3.055 \cdot 10^{-3} \cdot N_G + (0.06881 \cdot \varphi_V^2 - 0.03754 \cdot \varphi_V) + MS^{AP} \quad (29)$$

$$MS^{AP} = p_S \cdot [-1.314617 - 9.614 \cdot 10^{-4} \cdot N_G - 0.4687 \cdot (0.07063 \cdot \varphi_V^2 - 0.09766 \cdot \varphi_V)] \quad (30)$$

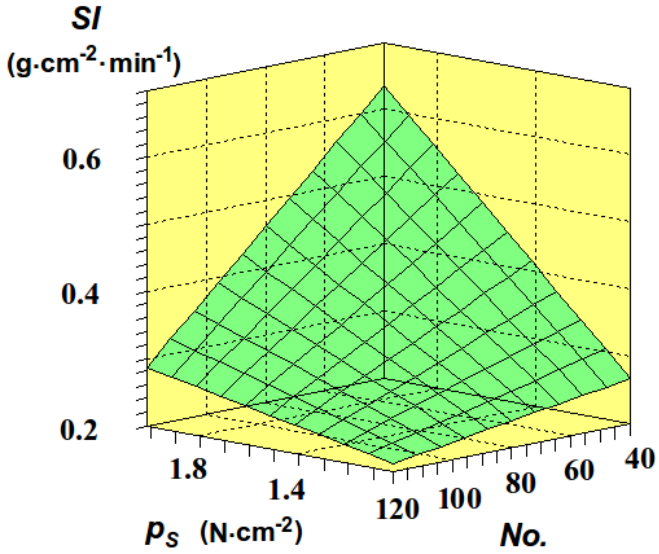

Fig. 20. The impact of the specific sanding intensity *SI* (g·cm^{-2}·min^{-1}) and the sanding pressure p_S (N·cm^{-2}) and the number of sanding grit N_G, according to formula (29)-(30); sanding parameters: φ_V=60°, *D*=619 kg·m^{-3}, R_T=820 kG·cm^{-2}, R_S=90 kG·cm^{-2}, R_C=490 kG·cm^{-2}, R_B=950 kG·cm^{-2}, *E*= 94·10^3 kG·cm^{-2} (*Acer pseudoplatanus* L.)

The plot in Fig. 21, according to formula (31)-(32), for wood of ***Alnus glutinosa* Gaertn.**, showed that the maximum and minimum values of the sanding intensity *SI* (g·cm^{-2}·min^{-1}), as high as *SI*=1.06 g·cm^{-2}·min^{-1} and *SI*=0.41 g·cm^{-2}·min^{-1}, were larger, by as much as 12% and 55%, respectively, in comparison to the *Pinus sylvestris* L. wood specimen. Explanation of these observations might be the fact that all of physical and mechanical properties of *Alnus glutinosa* Gaertn. were lower in comparison to the wood of *Pinus sylvestris* L.

$$SI^{AG} = -0.393759 + 3.055 \cdot 10^{-3} \cdot N_G + (0.06881 \cdot \varphi_V^2 - 0.03754 \cdot \varphi_V) + MS^{AG} \quad (31)$$

$$MS^{AG} = p_S \cdot [0.778738 - 9.614 \cdot 10^{-4} \cdot N_G - 0.4687 \cdot (0.07063 \cdot \varphi_V^2 - 0.09766 \cdot \varphi_V)] \quad (32)$$

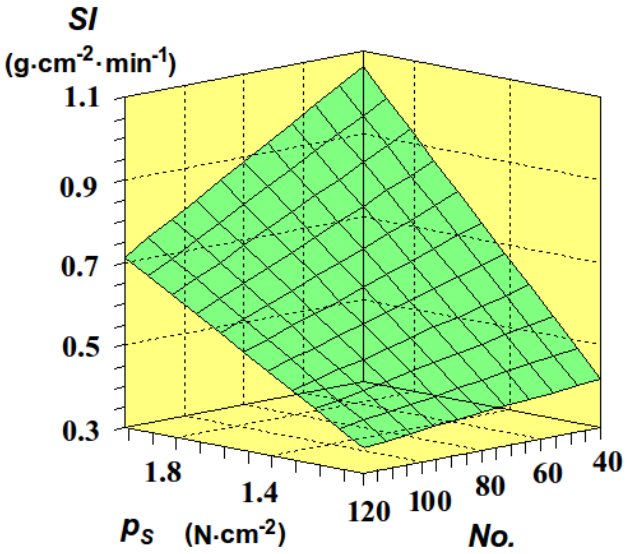

Fig. 21. The impact of the specific sanding intensity *SI* (g·cm^{-2}·min^{-1}) and the sanding pressure p_S, (N·cm^{-2}) and the number of sanding grit N_G, according to formula (31)-(32); sanding parameters: φ_V=60º, *D*=528 kg·m^{-3}, R_T=940 kG·cm^{-2}, R_S=51 kG·cm^{-2}, R_C=400 kG·cm^{-2}, R_B=970 kG·cm^{-2}, *E*=106·10^3 kG·cm^{-2} (*Alnus glutinosa* Gaertn.)

Figures 17 to 21 show that the specific sanding intensity *SI* (g·cm^{-2}·min^{-1}), by the grain angle φ_V=60º was the largest for sanding, with use of sanding grit number N_G=40, for all examined wood species. The impact of properties of wood specimens examined on the specific belt sanding intensity *SI* (g·cm^{-2}·min^{-1}) were not clear. The largest maximum of the intensity *SI* (g·cm^{-2}·min^{-1}) of 1.06 g·cm^{-2}·min^{-1} was observed for wood of *Alnus glutinosa* Gaertn., by the lowest density *D* (kg·m^{-3}) of 528 kg·cm^{-3}, but the lowest maximum of the *SI* (g·cm^{-2}·min^{-1}) of 0.64 g·cm^{-2}·min^{-1} was not observed for wood of the largest density. The largest minimum of the *SI* (g·cm^{-2}·min^{-1}) of 0.36 g·cm^{-2}·min^{-1} was observed for the wood of *Alnus glutinosa* Gaertn., by the lowest density *D* (kg·m^{-3}) of 528 kg·cm^{-3}, but the lowest minimum of the *SI* (g·cm^{-2}·min^{-1}) of 0.13 g·cm^{-2}·min^{-1} was not observed for wood of the largest density. More experiments are needed to explain this influence.

The influence of the wood grain angle φ_V (º) and the sanding pressure p_S (N·cm^{-2}) on the specific sanding intensity *SI* (g·cm^{-2}·min^{-1}), for wood of ***Pinus sylvestris* L.**, according to formulas (23)-(24) is shown in Fig. 22. An increase of the wood grain angle φ_V (º) from φ_V=0º to φ_V=90º, by the largest sanding pressure p_S=2.02 N·cm^{-2}, increased the specific sanding intensity *SI* (g·cm^{-2}·min^{-1}), from *SI* =0.88 g·cm^{-2}·min^{-1} to *SI* =1.02 g·cm^{-2}·min^{-1}. An increase of the grain angle φ_V from φ_V =0º to φ_V =90º, by the smallest sanding pressure p_S =1.02 N·cm^{-2}, increased less the specific sanding intensity *SI* (g·cm^{-2}·min^{-1}), from *SI* =0.14 g·cm^{-2}·min^{-1} to *SI* =0.28 g·cm^{-2}·min^{-1}. The general shape of influence of the wood grain angle φ_V (º) and the sanding pressure p_S (N·cm^{-2}) on the specific sanding intensity *SI* (g·cm^{-2}·min^{-1}), was similar for all wood specimens examined.

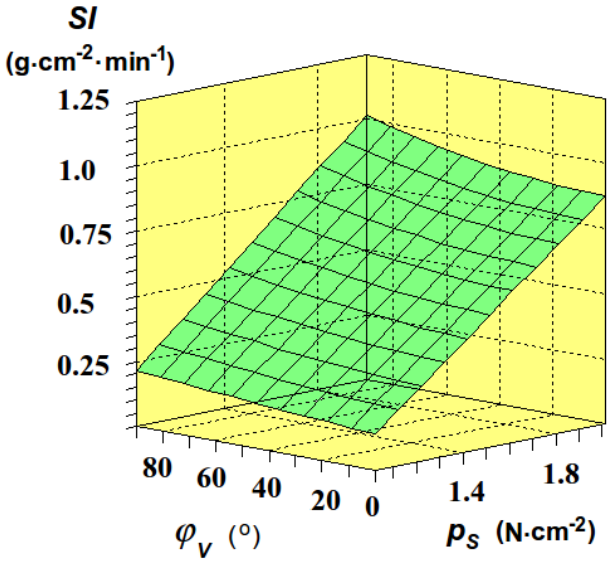

Fig. 22. Dependence between the specific sanding intensity *SI* (g·cm^{-2}·min^{-1}) and the sanding pressure p_S (N·cm^{-2}) and the wood grain angle φ_V (°), according to formula (23)-(24); sanding parameters: N_G=40, D=551 kg·m^{-3}, R_R=1040 kG·cm^{-2}, R_T=100 kG·cm^{-2}, R_C=435 kG·cm^{-2}, R_G=1000 kG/cm^2, E=120·10^3 kG·cm^{-2} (*Pinus sylvestris* L.)

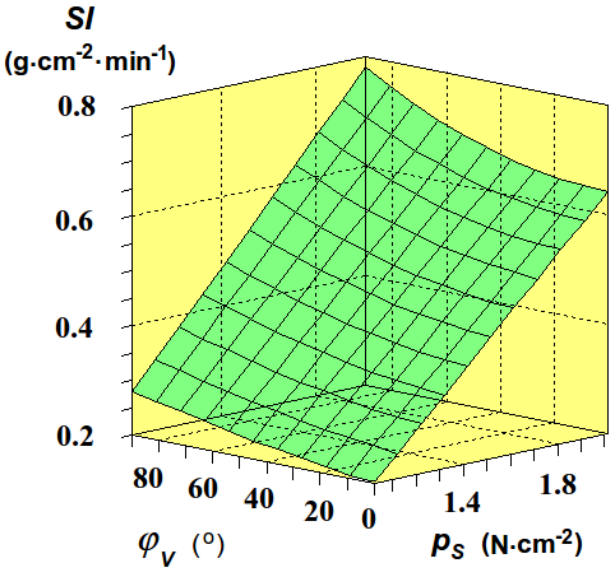

Fig. 23. The impact of the specific sanding intensity *SI* (g·cm^{-2}·min^{-1}) and the sanding pressure p_S (N·cm^{-2}) and the wood grain angle φ_V (°), according to formula (25)-(26); sanding parameters: N_G=40, D=540 kg·m^{-3}, R_T=500 kG·cm^{-2}, R_S=67 kG·cm^{-2}, R_C=430 kG·cm^{-2}, R_B=780 kG·cm^{-2}, E=110·10^3 kG·cm^{-2} (*Picea abies* L.)

The plot in Fig. 23, according to formulas (25)-(26), for wood of *Picea abies* L., showed that the maximum value of the *SI* (g·cm^{-2}·min^{-1}), as high as *SI*=0.78 g·cm^{-2}·min^{-1} was smaller, by as much as 23% in comparison to *Pinus sylvestris* L. wood, while the minimum value of the *SI* (g·cm^{-2}·min^{-1}), as high as *SI*=0.2 g·cm^{-2}·min^{-1} was higher, by as much as 30% in comparison to *Pinus sylvestris* L. wood.

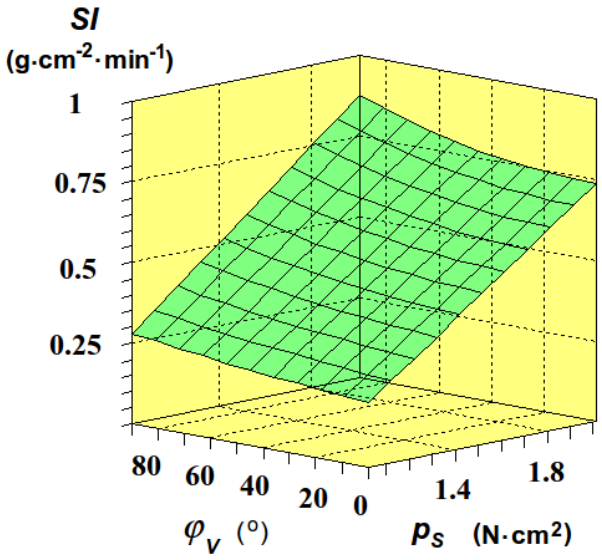

Fig. 24. The impact of the specific sanding intensity *SI* (g·cm^{-2}·min^{-1}) and the sanding pressure p_S (N·cm^{-2}) and the wood grain angle φ_V (°), according to formula (27)-(28); sanding parameters: N_G=40, D=744 kg·m^{-3}, R_T=900 kG·cm^{-2}, R_S=75 kG·cm^{-2}, R_C=470 kG·cm^{-2}, R_B=880 kG·cm^{-2}, E=117·10^3 kG·cm^{-2} (*Quercus robra* L.)

The plot in Fig. 24, according to formula (27)-(28), for the wood of ***Quercus robra* L.**, showed that maximum value of the *SI* (g·cm^{-2}·min^{-1}), as high as *SI*=0.88 g·cm^{-2}·min^{-1} was smaller, by as much as 14 % in comparison to *Pinus sylvestris* L., while the minimum value as high as *SI*=0.2 g·cm^{-2}·min^{-1} was higher, by as much as 30 % in comparison to *Pinus sylvestris* L. wood specimen.

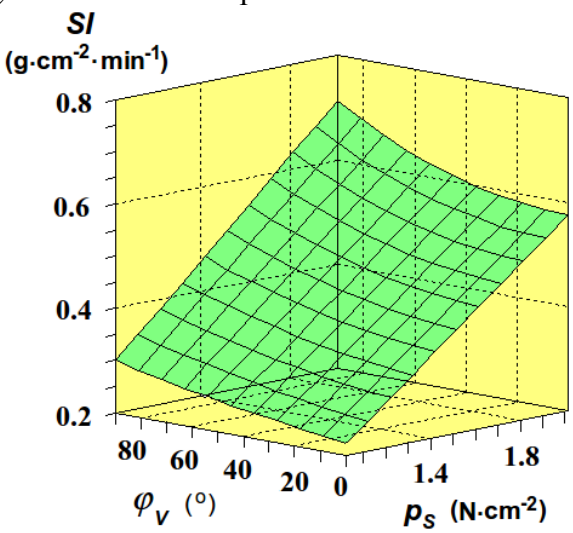

Fig. 25. The impact of the specific sanding intensity *SI* (g·cm^{-2}·min^{-1}) and the sanding pressure p_S (N·cm^{-2}), and the wood grain angle φ_V (°), according to formula (29)-(30); sanding parameters: N_G=40, D=619 kg·m^{-3}, R_T=820 kG·cm^{-2}, R_S=90 kG·cm^{-2}, R_C=490 kG·cm^{-2}, R_B=950 kG·cm^{-2}, E= 94·10^3 kG·cm^{-2} (*Acer pseudoplatanus* L.)

The plot in Fig. 25, according to formula (29)-(30), for *Acer pseudoplatanus* L. wood, illustrated that the maximum value of the *SI*, as high as *SI*=0.71 g·cm^{-2}·min^{-1} was smaller, by as much as 30% in comparison to *Pinus sylvestris* L., while the minimum value of the *SI* (g·cm^{-2}·min^{-1}), as high as *SI*=0.22 g·cm^{-2}·min^{-1} was higher, as much as 37 % in comparison to *Pinus sylvestris* L. wood specimen.

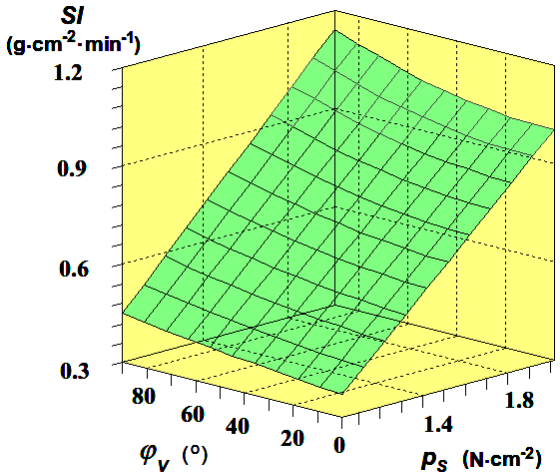

Fig. 26. The impact of the specific sanding intensity *SI* (g·cm^{-2}·min^{-1}) and the sanding pressure p_S (N·cm^{-2}), the wood grain angle φ_V (°), according to formula (31)-(32); sanding parameters: N_G=40, *D*=528 kg·m^{-3}, R_T=940 kG·cm^{-2}, R_S=51 kG·cm^{-2}, R_C=400 kG·cm^{-2}, R_B=970 kG·cm^{-2}, *E*=106·10^3 kG·cm^{-2} (*Alnus glutinosa* Gaertn.)

The plot in Fig. 26, according to formula (31)-(32) for wood of ***Alnus glutinosa* Gaertn.**, showed that the maximum and minimum values of the *SI* (g·cm^{-2}·min^{-1}), as high as *SI*=1.0 g·cm^{-2}·min^{-1} and *SI*=0.37 g·cm^{-2}·min^{-1} were larger, by as much as 12% and 62%, respectively, in comparison to *Pinus sylvestris* L. wood specimen.

Figures 22 to 26 illustrated that the specific sanding intensity *SI* (g·cm^{-2}·min^{-1}) was larger for transversely sanding, by angle φ_V=90°, in comparison to sanding parallel to wood, grains by angle φ_V=0°, for all examined wood species.

Properties of wood specimens examined taken into account had complex influence on the specific sanding intensity *SI* (g·cm^{-2}·min^{-1}). They did not follow each other. For example the largest maximum intensity *SI* (g·cm^{-2}·min^{-1}) of 1.14 g·cm^{-2}·min^{-1} was observed for the wood of *Alnus glutinosa* Gaertn., by the lowest wood density *D* (kg·m^{-3}), but the lowest maximum of intensity *SI* (g·cm^{-2}·min^{-1}) of 0.71 g·cm^{-2}·min^{-1} was observed for wood of *Acer pseudoplatanus* L., not by the largest wood density *D* (kg·m^{-3}) of 619 kg·m^{-3}. Although the difference in average wood density between *Quercus robra* L and *Acer pseudoplatanus* L. was significant, the explanation might be the presence of large pores in the wood of *Quercus robra* L, which are not present in the wood of *Acer pseudoplatanus* L. Also the average values of the R_S (kG·cm^{-2}), R_C (kG·cm^{-2}), R_B (kG·cm^{-2}) and *E* (kG·cm^{-2}) of the *Acer pseudoplatanus* L. were slightly higher in comparison to the wood of *Quercus robra* L. The wood density seemed to have less influence on the specific sanding intensity *SI* (g·cm^{-2}·min^{-1}) than the R_S (kG·cm^{-2}), R_C (kG·cm^{-2}), R_B (kG·cm^{-2}) and *E* (kG·cm^{-2}) wood properties.

The Influence of Sanding Parameters on the Elastic Feed Speed vF

For formula (8)-(9), describing the dependency of the average, elastic feed speed $v_F=f(p_S, N_G, \varphi_V, D, R_T, R_S, R_C, R_B, E)$ (mm·min^{-1}), the following estimators were evaluated: c_1=2.121, c_2=-0.47525, c_3=4.8·10^{-3}, c_4=2.87·10^{-4}, c_5=12.85031, c_6=-1.33·10^{-5}, c_7=-2.51·10^{-3}, c_8=-4.67·10^{-3}, c_9=7.33·10^{-4}, c_{10}=1.08·10^{-4}, c_{11}=-5.47·10^{-6}, c_{12}=1.4·10^{-3}, c_{13}=1.37·10^{-5}, c_{14}=1.0246, c_{15}=1.93·10^{-3}, c_{16}=-6.27·10^{-3}, c_{17}=-8.07·10^{-4}, and c_{18}=-3.6·10^{-3}. The quality of approximation of the fit of the formula (8)-(9) was characterized by the quantifiers: S_K=5.56, R=0.93, R^2=0.86, S_D=0.18 mm·min^{-1}. The coefficients of relatively importance C_{RI} for estimators of formula (4)-(5) were as follows: C_{RI1}=14238, C_{RI2}=1852, C_{RI3}=549, C_{RI4}=10, C_{RI5}=10, C_{RI6}=0.2, C_{RI7}=16942, C_{RI8}=419, C_{RI9}=339, C_{RI10}=31, C_{RI11}=1136, C_{RI13}=13493, C_{RI14}=17, C_{RI15}=18360, C_{RI15}=8197, C_{RI16}=2430, C_{RI17}=1846, and C_{RI18}=21139. The relation $v_F=f(p_S, N_G, \varphi_V, D, R_T, R_S, R_C, R_B, E)$ (mm·min^{-1}) plot is similar to $SI=f(p_S, N_G, \varphi_V, D, R_T, R_S, R_C, R_B, E)$ (g·cm^{-2}·min^{-1}) presented above.

CONCLUSIONS

Results from the analysis of the experiments performed showed that:

1. The specific belt sanding resistance K (N·cm^{-2}) strongly depends upon sanding pressure p_S. An increase of the sanding pressure p_S (N·cm^{-2}) increased the specific sanding resistance K (N·cm^{-2}), with the exception of *Populus nigra* L. wood specimen and grit number N_G>40.
2. The impact of sanding pressure p_S (N·cm^{-2}) on the specific belt sanding resistance K (N·cm^{-2}) not follow properties of wood specimens examined.
3. An augmentation of the sanding grit number N_G increased the specific sanding resistance K (N·cm^{-2}) for all wood species examined, with the exception of *Populus nigra* L. wood specimen, but to a lesser degree in comparison to the influence of the sanding pressure p_S (N·cm^{-2}).
4. The influence of the wood grain angle φ_V (°), on the specific sanding resistance K (N·cm^{-2}) was very complex, with several extremes.
5. In the relation between wood grains angle φ_V (°), and specific sanding resistance K (N·cm^{-2}), for the lowest sanding pressure p_S=1.02 N·cm^{-2} two minima at angle φ_V=0° and φ_V=90°, and one maximum, at angle φ_V=47° were found.
6. In the relation between wood grains angle φ_V (°), and specific sanding resistance K (N·cm^{-2}), by the largest sanding pressure p_S=2.01 N·cm^{-2}, two maxima, at angles φ_V=0° and φ_V=90°, and one minimum, at angle φ_V=40° were found.
7. The extremenesses in relation $K=f(\varphi_V)$ (N·cm^{-2}) mentioned on pages 1638-1641 (Figs. 10-15) disappeared when applying a sanding pressure of at least p_S=1.82 N·cm^{-2}.
8. The specific sanding resistance K (N·cm^{-2}), for transversely sanding, by angles φ_V=90° was slightly higher in comparison to sanding parallel to wood grains by angle φ_V=0°, for all examined wood specimens.

9. The specific belt sanding intensity SI ($g \cdot cm^{-2} \cdot min^{-1}$) strongly depends upon sanding pressure p_S ($N \cdot cm^{-2}$). An increase of the sanding pressure p_S ($N \cdot cm^{-2}$) enlarged the specific sanding intensity SI ($g \cdot cm^{-2} \cdot min^{-1}$) for all wood species examined.
10. An increase of the sanding grit number N_G decreased the specific sanding intensity SI ($g \cdot cm^{-2} \cdot min^{-1}$) for all wood specimens.
11. An increase of the wood grain angle φ_V (°), in whole range of variation slightly enlarged the specific sanding intensity SI ($g \cdot cm^{-2} \cdot min^{-1}$) for all wood specimens.
12. The specific sanding intensity SI ($g \cdot cm^{-2} \cdot min^{-1}$) did not follow wood density and other mechanical properties analyzed in this study.

ACKNOWLEDGMENTS

The authors are grateful for the support of the Poznań Networking & Supercomputing Center (PCSS) calculation grant.

REFERENCES CITED

Banski, A. (2004). "Fyzikálno-mechanické javy drevo-nástroj v procese brusenia rastlého dreva.," PhD thesis, Zvolen, (in Slovakian).

Banski, A. (2000). "Technicke vlasnosti brusneho prostredku a vykon pri bruseni dreva.," *Proc. Woodtech*, Trencin, Zvolen ES TU, 157-164, (in Slovakian).

Banský, M., Naščak, L., Wieloch G. (1999). "Testovanie brúsnych papierov z hľadiska ich živostnosti.," Proc. I MVK "Stroj-nástroj-obrobok," Nitra, October, 19-22, (in Slovakian).

Bansky, M., Nascak, L., and Wieloch G. (2000). "Vplyv brusnej rýchlosti na teplotu brusneho povrchu a výsku odbrusu pri bruseni buka brusnymi papermi s roznou zrnitostou.," Proc. II MVK "Trieskove a beztrieskove obrabeni dreva," *Stary Smokovec*, Zvolen, ES TU, 13-18, (in Slovakian).

Barcik, S., and Vacek, V. (1999). "Experimentálne sledovanie vplyvu brúsenia dreva na energetickú spotrebu a vzťažny odbrus," *Acta Facultatis Xylologial*, Zvolen, TU.

Lisndgren, B., and Norin, T. (1969). "Hartseskemi. Hartskompendium," Stockholm, Svenska Papers och Cellulosa Ingenioersfoereningen, 20-29, (in Swedish).

Matsumoto, H. A., and Murase, Y. (1999). "The effects of sanding pressure and grit size on both AE and sanding performance in disc sanding process," Proc. 14th International Wood Machining Seminar V.2, Paris-Epinal-Cluny, France, 653-662.

Očkajová, A. (2002). "Analýza faktorov v procese plošného brúsenia dreva.," Vedecká štúdia 4/2002/A, ES TU Zvolen, (in Slovakian).

Pahllitzsch, G., and Dziobek, K. (1959). "Untersuchungen über das Bandschleifen von Holz mit geradliniger Schnittbedingungen," *Holz als Roh und Werkstoff* V17, 121-134, (in German).

Pahllitzsch, G., and Dziobek, K. (1961). "Über das Wesen der Abstumpfung von Schleifenbänder beim Bandschleifen von Holz," *Holz als Roh und Werkstoff* V19, 136-149, (in German).

Porankiewicz, B. (1988). "Mathematical model of edge dullness for prediction of wear of wood cutting tool," *9 Wood Machining Seminar*, University of California, Forest Products Laboratory, Richmond, USA, 169-170.

Porankiewicz, B., and Wieloch, G. (2008). "Sanding of *Fagus silvatica L.* wood perpendicularly to grains," *BioResources,* http://www.ncsu.edu/bioresources/index.htm, ISSN: 1930-2126, no. 3(3), 684-700.

Taylor, J. B., Carrano A. L., and Lemaster R. L. (1999). "Experimental modelling of the sanding process. The relationship between input and output parameters," Proc. 14th International Wood Machining Seminar, Paris-Epinal-Cluny, France, V. 1: 73-82.

Wagenfür, R., and Scheiber, C. (1974). "Holzatlas," *VEB Fachbuchverlag*, Leipzig, (in German).

Article submitted: April 28, 2010; peer review completed: June 1, 2010; revised version received: June 4, 2010; accepted: June 13, 2010; published: June 15, 2010.

APPENDIX

Table 2A. Experimental Matrix for Specific Sanding Resistance K (N·cm^{-2})

No.	p_S (N·cm^{-2})	N_O	φ_V (º)	D (kg·m^{-3})	R_{RII}	R_T (KG·cm^{-2})	R_{CII}	R_G	$E\cdot10^{-3}$	K (N·cm^{-2})
1	1.02	40	60	551	1040	100	435	1000	120	0.883
2	1.02	40	0	551	1040	100	435	1000	120	0.869
3	1.02	40	90	551	1040	100	435	1000	120	0.882
4	1.02	80	60	551	1040	100	435	1000	120	0.920
5	1.02	80	0	551	1040	100	435	1000	120	0.938
6	1.02	80	90	551	1040	100	435	1000	120	0.887
7	1.02	120	60	551	1040	100	435	1000	120	1.032
8	1.02	120	0	551	1040	100	435	1000	120	1.022
9	1.02	120	90	551	1040	100	435	1000	120	1.077
10	1.43	40	60	551	1040	100	435	1000	120	1.250
11	1.43	40	0	551	1040	100	435	1000	120	1.114
12	1.43	40	90	551	1040	100	435	1000	120	1.173
13	1.43	80	60	551	1040	100	435	1000	120	1.176
14	1.43	80	0	551	1040	100	435	1000	120	1.345
15	1.43	80	90	551	1040	100	435	1000	120	1.255
16	1.43	120	60	551	1040	100	435	1000	120	1.232
17	1.43	120	0	551	1040	100	435	1000	120	1.401
18	1.43	120	90	551	1040	100	435	1000	120	1.336
19	1.83	40	60	551	1040	100	435	1000	120	1.381
20	1.83	40	0	551	1040	100	435	1000	120	1.445
21	1.83	40	90	551	1040	100	435	1000	120	1.277
22	1.83	80	60	551	1040	100	435	1000	120	1.156
23	1.83	80	0	551	1040	100	435	1000	120	1.778
24	1.83	80	90	551	1040	100	435	1000	120	1.654
25	1.83	120	60	551	1040	100	435	1000	120	1.623
26	1.83	120	0	551	1040	100	435	1000	120	1.533
27	1.83	120	90	551	1040	100	435	1000	120	1.538
28	2.02	40	60	551	1040	100	435	1000	120	1.254
29	2.02	40	0	551	1040	100	435	1000	120	1.132
30	2.02	80	60	551	1040	100	435	1000	120	1.260
31	2.02	80	0	551	1040	100	435	1000	120	1.643
32	2.02	80	90	551	1040	100	435	1000	120	1.511
33	2.02	120	0	551	1040	100	435	1000	120	1.685
34	2.02	120	90	551	1040	100	435	1000	120	1.337
35	1.02	40	60	450	900	67	430	780	110	0.646
36	1.02	40	0	450	900	67	430	780	110	0.851
37	1.02	40	90	450	900	67	430	780	110	0.706
38	1.02	80	60	450	900	67	430	780	110	0.671
39	1.02	80	0	450	900	67	430	780	110	0.602
40	1.02	80	90	450	900	67	430	780	110	0.694
41	1.02	120	60	450	900	67	430	780	110	0.869
42	1.02	120	0	450	900	67	430	780	110	0.792
43	1.02	120	90	450	900	67	430	780	110	0.811

Table 2B. Experimental Matrix for Specific Sanding Resistance K (N·cm^{-2})

No.	p_S (N·cm^{-2})	N_O	φ_V (°)	D (kg·m^{-3})	R_{RII}	R_T (KG·cm^{-2})	R_{CII}	R_G	$E \cdot 10^{-3}$	K (N·cm^{-2})
44	1.43	40	60	450	900	67	430	780	110	1.095
45	1.43	40	0	450	900	67	430	780	110	0.943
46	1.43	40	90	450	900	67	430	780	110	0.854
47	1.43	80	60	450	900	67	430	780	110	0.907
48	1.43	80	0	450	900	67	430	780	110	1.004
49	1.43	80	90	450	900	67	430	780	110	1.102
50	1.43	120	60	450	900	67	430	780	110	1.064
51	1.43	120	0	450	900	67	430	780	110	1.108
52	1.43	120	90	450	900	67	430	780	110	1.003
53	1.83	40	60	450	900	67	430	780	110	1.107
54	1.83	40	0	450	900	67	430	780	110	1.128
55	1.83	40	90	450	900	67	430	780	110	0.941
56	1.83	80	60	450	900	67	430	780	110	1.265
57	1.83	80	0	450	900	67	430	780	110	1.152
58	1.83	80	90	450	900	67	430	780	110	1.450
59	1.83	120	60	450	900	67	430	780	110	1.605
60	1.83	120	0	450	900	67	430	780	110	1.436
61	1.83	120	90	450	900	67	430	780	110	1.410
62	2.02	40	60	450	900	67	430	780	110	1.241
63	2.02	40	0	450	900	67	430	780	110	1.615
64	2.02	40	90	450	900	67	430	780	110	1.293
65	2.02	80	60	450	900	67	430	780	110	1.413
66	2.02	80	0	450	900	67	430	780	110	1.509
67	2.02	80	90	450	900	67	430	780	110	1.405
68	2.02	120	60	450	900	67	430	780	110	1.486
69	2.02	120	0	450	900	67	430	780	110	1.453
70	2.02	120	90	450	900	67	430	780	110	1.454
71	1.02	40	60	744	900	75	470	880	117	0.887
72	1.02	40	0	744	900	75	470	880	117	0.574
73	1.02	40	90	744	900	75	470	880	117	0.584
74	1.02	80	60	744	900	75	470	880	117	1.068
75	1.02	80	0	744	900	75	470	880	117	0.576
76	1.02	80	90	744	900	75	470	880	117	0.627
77	1.02	120	60	744	900	75	470	880	117	1.266
78	1.02	120	0	744	900	75	470	880	117	0.833
79	1.02	120	90	744	900	75	470	880	117	0.776
80	1.43	40	60	744	900	75	470	880	117	1.572
81	1.43	40	0	744	900	75	470	880	117	1.164
84	1.43	40	90	744	900	75	470	880	117	1.185
83	1.43	80	60	744	900	75	470	880	117	1.353
84	1.43	80	0	744	900	75	470	880	117	1.347
85	1.43	80	90	744	900	75	470	880	117	1.306
86	1.43	120	60	744	900	75	470	880	117	1.480
87	1.43	120	0	744	900	75	470	880	117	1.281
88	1.43	120	90	744	900	75	470	880	117	1.263

Table 2C. Experimental Matrix for Specific Sanding Resistance K (N·cm^{-2})

No.	p_S (N·cm^{-2})	N_O	φ_V (°)	D (kg·m^{-3})	R_{RII}	R_T (KG·cm^{-2})	R_{CII}	R_G	$E \cdot 10^{-3}$	K (N·cm^{-2})
89	1.83	40	60	744	900	75	470	880	117	1.730
90	1.83	40	0	744	900	75	470	880	117	1.561
91	1.83	40	90	744	900	75	470	880	117	1.655
92	1.83	80	60	744	900	75	470	880	117	1.753
93	1.83	80	0	744	900	75	470	880	117	1.769
94	1.83	80	90	744	900	75	470	880	117	1.637
95	1.83	120	60	744	900	75	470	880	117	1.833
96	1.83	120	0	744	900	75	470	880	117	1.546
97	1.83	120	90	744	900	75	470	880	117	1.478
98	2.02	40	60	744	900	75	470	880	117	1.934
99	2.02	40	0	744	900	75	470	880	117	2.033
100	2.02	40	90	744	900	75	470	880	117	2.082
101	2.02	80	60	744	900	75	470	880	117	1.747
102	2.02	80	0	744	900	75	470	880	117	1.474
103	2.02	80	90	744	900	75	470	880	117	1.825
104	2.02	120	60	744	900	75	470	880	117	1.629
105	2.02	120	0	744	900	75	470	880	117	1.924
106	2.02	120	90	744	900	75	470	880	117	1.502
107	1.02	40	60	619	820	90	490	950	94	0.883
108	1.02	40	0	619	820	90	490	950	94	0.869
109	1.02	40	90	619	820	90	490	950	94	0.882
110	1.02	80	60	619	820	90	490	950	94	0.920
111	1.02	80	0	619	820	90	490	950	94	0.938
112	1.02	80	90	619	820	90	490	950	94	0.887
113	1.02	120	60	619	820	90	490	950	94	1.032
114	1.02	120	0	619	820	90	490	950	94	1.022
115	1.02	120	90	619	820	90	490	950	94	1.077
116	1.43	40	60	619	820	90	490	950	94	1.301
117	1.43	40	0	619	820	90	490	950	94	1.254
118	1.43	40	90	619	820	90	490	950	94	1.265
119	1.43	80	60	619	820	90	490	950	94	1.173
120	1.43	80	0	619	820	90	490	950	94	1.106
121	1.43	80	90	619	820	90	490	950	94	1.153
122	1.43	120	60	619	820	90	490	950	94	1.434
123	1.43	120	0	619	820	90	490	950	94	1.098
124	1.43	120	90	619	820	90	490	950	94	1.176
125	1.83	40	60	619	820	90	490	950	94	1.688
126	1.83	40	0	619	820	90	490	950	94	1.738
127	1.83	40	90	619	820	90	490	950	94	1.680
128	1.83	80	60	619	820	90	490	950	94	1.457
129	1.83	80	0	619	820	90	490	950	94	1.469
130	1.83	80	90	619	820	90	490	950	94	1.546
131	1.83	120	60	619	820	90	490	950	94	1.676
132	1.83	120	0	619	820	90	490	950	94	1.320
133	1.83	120	90	619	820	90	490	950	94	1.556

Table 2D. Experimental Matrix for Specific Sanding Resistance K (N·cm^{-2})

No.	p_S (N·cm^{-2})	N_O	φ_V (°)	D (kg·m^{-3})	R_{RII}	R_T (KG·cm^{-2})	R_{CII}	R_G	$E \cdot 10^{-3}$	K (N·cm^{-2})
134	2.02	40	60	619	820	90	490	950	94	1.689
135	2.02	40	0	619	820	90	490	950	94	1.614
136	2.02	40	90	619	820	90	490	950	94	1.643
137	2.02	80	60	619	820	90	490	950	94	1.498
138	2.02	80	0	619	820	90	490	950	94	1.476
139	2.02	80	90	619	820	90	490	950	94	1.628
140	2.02	120	60	619	820	90	490	950	94	1.401
141	2.02	120	0	619	820	90	490	950	94	1.827
142	2.02	120	90	619	820	90	490	950	94	1.586
143	1.02	40	60	528	940	51	400	970	106	0.875
144	1.02	40	0	528	940	51	400	970	106	0.765
145	1.02	40	90	528	940	51	400	970	106	0.885
146	1.02	80	60	528	940	51	400	970	106	0.962
147	1.02	80	0	528	940	51	400	970	106	0.841
148	1.02	80	90	528	940	51	400	970	106	0.973
149	1.02	120	60	528	940	51	400	970	106	1.125
150	1.02	120	0	528	940	51	400	970	106	0.9851
151	1.02	120	90	528	940	51	400	970	106	1.138
152	1.43	40	60	528	940	51	400	970	106	0.897
153	1.43	40	0	528	940	51	400	970	106	0.845
154	1.43	40	90	528	940	51	400	970	106	0.923
155	1.43	80	60	528	940	51	400	970	106	1.286
156	1.43	80	0	528	940	51	400	970	106	1.029
157	1.43	80	90	528	940	51	400	970	106	1.315
158	1.43	120	60	528	940	51	400	970	106	1.253
159	1.43	120	0	528	940	51	400	970	106	1.186
160	1.43	120	90	528	940	51	400	970	106	1.387
161	1.83	40	60	528	940	51	400	970	106	1.232
162	1.83	40	0	528	940	51	400	970	106	1.103
163	1.83	40	90	528	940	51	400	970	106	1.345
164	1.83	80	60	528	940	51	400	970	106	1.315
165	1.83	80	0	528	940	51	400	970	106	1.303
166	1.83	80	90	528	940	51	400	970	106	1.439
167	1.83	120	60	528	940	51	400	970	106	1.454
168	1.83	120	0	528	940	51	400	970	106	1.40
169	1.83	120	90	528	940	51	400	970	106	1.578
170	2.02	40	60	528	940	51	400	970	106	1.145
171	2.02	40	0	528	940	51	400	970	106	1.026
172	2.02	40	90	528	940	51	400	970	106	1.263
173	2.02	80	60	528	940	51	400	970	106	1.639
174	2.02	80	0	528	940	51	400	970	106	1.618
175	2.02	80	90	528	940	51	400	970	106	1.759
176	2.02	120	60	528	940	51	400	970	106	1.834
176	2.02	120	0	528	940	51	400	970	106	1.742
178	2.02	120	90	528	940	51	400	970	106	1.934

Table 2E. Experimental Matrix for Specific Sanding Resistance K (N·cm^{-2})

No.	p_S (N·cm^{-2})	N_O	φ_V (°)	D (kg·m^{-3})	R_{RII}	R_T (KG·cm^{-2})	R_{CII}	R_G	$E \cdot 10^{-3}$	K (N·cm^{-2})
179	1.02	40	60	487	770	50	300	650	88	1.022
180	1.02	40	0	487	770	50	300	650	88	0.985
181	1.02	40	90	487	770	50	300	650	88	0.967
182	1.02	80	60	487	770	50	300	650	88	1.091
183	1.02	80	0	487	770	50	300	650	88	1.066
184	1.02	80	90	487	770	50	300	650	88	1.023
185	1.02	120	60	487	770	50	300	650	88	1.400
186	1.02	120	0	487	770	50	300	650	88	1.234
187	1.02	120	90	487	770	50	300	650	88	1.342
188	1.43	40	60	487	770	50	300	650	88	1.474
189	1.43	40	0	487	770	50	300	650	88	1.133
190	1.43	40	90	487	770	50	300	650	88	1.079
191	1.43	80	60	487	770	50	300	650	88	1.329
192	1.43	80	0	487	770	50	300	650	88	1.178
193	1.43	80	90	487	770	50	300	650	88	1.231
194	1.43	120	60	487	770	50	300	650	88	1.034
195	1.43	120	0	487	770	50	300	650	88	1.083
196	1.43	120	90	487	770	50	300	650	88	1.036
197	1.83	40	60	487	770	50	300	650	88	1.500
198	1.83	40	0	487	770	50	300	650	88	1.346
199	1.83	40	90	487	770	50	300	650	88	0.742
200	1.83	80	60	487	770	50	300	650	88	1.086
211	1.83	80	0	487	770	50	300	650	88	1.148
212	1.83	80	90	487	770	50	300	650	88	0.996
213	1.83	120	60	487	770	50	300	650	88	1.031
214	1.83	120	0	487	770	50	300	650	88	1.024
215	1.83	120	90	487	770	50	300	650	88	1.131
216	2.02	40	60	487	770	50	300	650	88	0.947
217	2.02	40	0	487	770	50	300	650	88	1.432
218	2.02	40	90	487	770	50	300	650	88	1.215
219	2.02	80	60	487	770	50	300	650	88	1.198
220	2.02	80	0	487	770	50	300	650	88	0.887
221	2.02	80	90	487	770	50	300	650	88	1.507
222	2.02	120	60	487	770	50	300	650	88	0.973
223	2.02	120	0	487	770	50	300	650	88	0.995
224	2.02	120	90	487	770	50	300	650	88	1.164

Table 3A. Experimental Matrix for Specific Sanding Intensity *SI* (g·cm^{-2}·min^{-1})

No.	p_S (N·cm^{-2})	N_O	ν (º)	*D* (kg·m^{-3})	R_{RII}	R_T	R_{CII} (kG·cm^{-2})	R_G	E·10^{-3}	*SI* (g·cm^{-2}·min^{-1})
1	1.02	40	60	551	1040	100	435	1000	120	0.262
2	1.02	40	0	551	1040	100	435	1000	120	0.198
3	1.02	40	90	551	1040	100	435	1000	120	0.232
4	1.02	80	60	551	1040	100	435	1000	120	0.244
5	1.02	80	0	551	1040	100	435	1000	120	0.114
6	1.02	80	90	551	1040	100	435	1000	120	0.126
7	1.02	120	60	551	1040	100	435	1000	120	0.243
8	1.02	120	0	551	1040	100	435	1000	120	0.133
9	1.02	120	90	551	1040	100	435	1000	120	0.105
10	1.43	40	60	551	1040	100	435	1000	120	0.470
11	1.43	40	0	551	1040	100	435	1000	120	0.453
12	1.43	40	90	551	1040	100	435	1000	120	0.589
13	1.43	80	60	551	1040	100	435	1000	120	0.335
14	1.43	80	0	551	1040	100	435	1000	120	0.287
15	1.43	80	90	551	1040	100	435	1000	120	0.352
16	1.43	120	60	551	1040	100	435	1000	120	0.282
17	1.43	120	0	551	1040	100	435	1000	120	0.315
18	1.43	120	90	551	1040	100	435	1000	120	0.314
19	1.83	40	60	551	1040	100	435	1000	120	0.780
20	1.83	40	0	551	1040	100	435	1000	120	0.807
21	1.83	40	90	551	1040	100	435	1000	120	0.741
22	1.83	80	60	551	1040	100	435	1000	120	0.621
23	1.83	80	0	551	1040	100	435	1000	120	0.424
24	1.83	80	90	551	1040	100	435	1000	120	0.527
25	1.83	120	60	551	1040	100	435	1000	120	0.493
26	1.83	120	90	551	1040	100	435	1000	120	0.451
27	2.02	40	60	551	1040	100	435	1000	120	0.988
28	2.02	40	0	551	1040	100	435	1000	120	1.207
29	2.02	40	90	551	1040	100	435	1000	120	1.172
30	2.02	120	60	551	1040	100	435	1000	120	0.618
31	2.02	120	0	551	1040	100	435	1000	120	0.549
32	2.02	120	90	551	1040	100	435	1000	120	0.672
33	2.02	80	60	551	1040	100	435	1000	120	1.217
34	1.83	120	0	551	1040	100	435	1000	120	0.450
35	2.02	80	0	551	1040	100	435	1000	120	1.404
36	2.02	80	90	551	1040	100	435	1000	120	1.636
37	1.02	40	60	450	900	67	430	780	110	0.346
38	1.02	40	0	450	900	67	430	780	110	0.2
39	1.02	40	90	450	900	67	430	780	110	0.315
40	1.02	80	60	450	900	67	430	780	110	0.165
41	1.02	80	0	450	900	67	430	780	110	0.135
42	1.02	80	90	450	900	67	430	780	110	0.191
43	1.02	120	60	450	900	67	430	780	110	0.165
44	1.02	120	0	450	900	67	430	780	110	0.088

Table 3B. Experimental Matrix for Specific Sanding Intensity *SI* (g·cm^{-2}·min^{-1})

No.	p_S (N·cm^{-2})	N_O	$_v$ (°)	*D* (kg·m^{-3})	R_{RII}	R_T	R_{CII} (kG·cm^{-2})	R_G	E·10^{-3}	*SI* (g·cm^{-2}·min^{-1})
45	1.02	120	90	450	900	67	430	780	110	0.142
46	1.43	40	60	450	900	67	430	780	110	0.449
47	1.43	40	0	450	900	67	430	780	110	0.293
48	1.43	40	90	450	900	67	430	780	110	0.524
49	1.43	80	60	450	900	67	430	780	110	0.318
50	1.43	80	0	450	900	67	430	780	110	0.410
51	1.43	80	90	450	900	67	430	780	110	0.610
52	1.43	120	60	450	900	67	430	780	110	0.217
53	1.43	120	0	450	900	67	430	780	110	0.218
54	1.43	120	90	450	900	67	430	780	110	0.381
55	1.83	40	60	450	900	67	430	780	110	0.653
56	1.83	40	0	450	900	67	430	780	110	0.460
57	1.83	40	90	450	900	67	430	780	110	0.787
58	1.83	80	60	450	900	67	430	780	110	0.460
59	1.83	80	0	450	900	67	430	780	110	0.469
60	1.83	80	90	450	900	67	430	780	110	0.634
61	1.83	120	60	450	900	67	430	780	110	0.253
62	1.83	120	0	450	900	67	430	780	110	0.207
63	1.83	120	90	450	900	67	430	780	110	0.336
64	2.02	40	60	450	900	67	430	780	110	0.706
65	2.02	40	0	450	900	67	430	780	110	0.658
66	2.02	40	90	450	900	67	430	780	110	0.932
67	2.02	80	60	450	900	67	430	780	110	0.461
68	2.02	80	0	450	900	67	430	780	110	0.475
69	2.02	80	90	450	900	67	430	780	110	0.581
70	2.02	120	60	450	900	67	430	780	110	0.254
71	2.02	120	0	450	900	67	430	780	110	0.259
72	2.02	120	90	450	900	67	430	780	110	0.326
73	1.02	40	60	744	900	75	470	880	117	0.146
74	1.02	40	0	744	900	75	470	880	117	0.207
75	1.02	40	90	744	900	75	470	880	117	0.214
76	1.02	80	60	744	900	75	470	880	117	0.156
77	1.02	80	0	744	900	75	470	880	117	0.228
78	1.02	80	90	744	900	75	470	880	117	0.232
79	1.02	120	60	744	900	75	470	880	117	0.148
80	1.02	120	0	744	900	75	470	880	117	0.227
81	1.02	120	90	744	900	75	470	880	117	0.275
82	1.43	40	60	744	900	75	470	880	117	0.310
83	1.43	40	0	744	900	75	470	880	117	0.503
84	1.43	40	90	744	900	75	470	880	117	0.535
85	1.43	80	60	744	900	75	470	880	117	0.269
86	1.43	80	0	744	900	75	470	880	117	0.415
87	1.43	80	90	744	900	75	470	880	117	0.468
88	1.43	120	60	744	900	75	470	880	117	0.234
89	1.43	120	0	744	900	75	470	880	117	0.381

Table 3C. Experimental Matrix for Specific Sanding Intensity *SI* (g·cm^{-2}·min^{-1})

No.	p_S (N·cm^{-2})	N_O	ν (°)	*D* (kg·m^{-3})	R_{RII}	R_T	R_{CII} (kG·cm^{-2})	R_G	E·10^{-3}	*SI* (g·cm^{-2}·min^{-1})
90	1.43	120	90	744	900	75	470	880	117	0.491
91	1.83	40	60	744	900	75	470	880	117	0.520
92	1.83	40	0	744	900	75	470	880	117	0.631
93	1.83	40	90	744	900	75	470	880	117	0.835
94	1.83	80	60	744	900	75	470	880	117	0.477
95	1.83	80	0	744	900	75	470	880	117	0.583
96	1.83	80	90	744	900	75	470	880	117	0.661
97	1.83	120	60	744	900	75	470	880	117	0.386
98	1.83	120	0	744	900	75	470	880	117	0.498
99	1.83	120	90	744	900	75	470	880	117	0.548
100	2.02	40	60	744	900	75	470	880	117	0.721
101	2.02	40	0	744	900	75	470	880	117	0.712
102	2.02	40	90	744	900	75	470	880	117	0.743
103	2.02	80	60	744	900	75	470	880	117	0.609
104	2.02	80	0	744	900	75	470	880	117	0.528
105	2.02	80	90	744	900	75	470	880	117	0.733
106	2.02	120	60	744	900	75	470	880	117	0.509
107	2.02	120	0	744	900	75	470	880	117	0.534
108	2.02	120	90	744	900	75	470	880	117	0.424
109	1.02	40	60	619	820	90	490	950	94	0.189
110	1.02	40	0	619	820	90	490	950	94	0.171
111	1.02	40	90	619	820	90	490	950	94	0.185
112	1.02	80	60	619	820	90	490	950	94	0.246
113	1.02	80	0	619	820	90	490	950	94	0.202
114	1.02	80	90	619	820	90	490	950	94	0.332
115	1.02	120	60	619	820	90	490	950	94	0.339
116	1.02	120	0	619	820	90	490	950	94	0.192
117	1.02	120	90	619	820	90	490	950	94	0.281
118	1.43	40	60	619	820	90	490	950	94	0.340
119	1.43	40	0	619	820	90	490	950	94	0.263
120	1.43	40	90	619	820	90	490	950	94	0.357
121	1.43	80	60	619	820	90	490	950	94	0.369
122	1.43	80	0	619	820	90	490	950	94	0.261
123	1.43	80	90	619	820	90	490	950	94	0.342
124	1.43	120	60	619	820	90	490	950	94	0.369
125	1.43	120	0	619	820	90	490	950	94	0.249
126	1.43	120	90	619	820	90	490	950	94	0.354
127	1.83	40	60	619	820	90	490	950	94	0.483
128	1.83	40	0	619	820	90	490	950	94	0.366
129	1.83	40	90	619	820	90	490	950	94	0.483
130	1.83	80	60	619	820	90	490	950	94	0.499
131	1.83	80	0	619	820	90	490	950	94	0.347
132	1.83	80	90	619	820	90	490	950	94	0.449
133	1.83	120	60	619	820	90	490	950	94	0.444
134	1.83	120	0	619	820	90	490	950	94	0.319

Table 3D. Experimental Matrix for Specific Sanding Intensity *SI* (g·cm^{-2}·min^{-1})

No.	p_S (N·cm^{-2})	N_O	ν (°)	*D* (kg·m^{-3})	R_{RII}	R_T	R_{CII} (kG·cm^{-2})	R_G	E·10^{-3}	*SI* (g·cm^{-2}·min^{-1})
135	1.83	120	90	619	820	90	490	950	94	0.450
136	2.02	40	60	619	820	90	490	950	94	0.554
137	2.02	40	0	619	820	90	490	950	94	0.454
138	2.02	40	90	619	820	90	490	950	94	0.524
139	2.02	80	60	619	820	90	490	950	94	0.497
140	2.02	80	0	619	820	90	490	950	94	0.407
141	2.02	80	90	619	820	90	490	950	94	0.521
142	2.02	120	60	619	820	90	490	950	94	0.434
143	2.02	120	0	619	820	90	490	950	94	0.273
144	2.02	120	90	619	820	90	490	950	94	0.521
145	1.02	40	60	528	940	51	400	970	106	0.537
146	1.02	40	0	528	940	51	400	970	106	0.458
147	1.02	40	90	528	940	51	400	970	106	0.556
148	1.02	80	60	528	940	51	400	970	106	0.487
149	1.02	80	0	528	940	51	400	970	106	0.241
150	1.02	80	90	528	940	51	400	970	106	0.502
151	1.02	120	60	528	940	51	400	970	106	0.220
152	1.02	120	0	528	940	51	400	970	106	0.209
153	1.02	120	90	528	940	51	400	970	106	0.312
154	1.43	40	60	528	940	51	400	970	106	0.790
155	1.43	40	0	528	940	51	400	970	106	0.643
156	1.43	40	90	528	940	51	400	970	106	0.758
157	1.43	80	60	528	940	51	400	970	106	0.724
158	1.43	80	0	528	940	51	400	970	106	0.485
159	1.43	80	90	528	940	51	400	970	106	0.690
160	1.43	120	60	528	940	51	400	970	106	0.401
161	1.43	120	0	528	940	51	400	970	106	0.272
162	1.43	120	90	528	940	51	400	970	106	0.548
163	1.83	40	60	528	940	51	400	970	106	1.071
164	1.83	40	0	528	940	51	400	970	106	0.835
165	1.83	40	90	528	940	51	400	970	106	1.019
166	1.83	80	60	528	940	51	400	970	106	0.962
167	1.83	80	0	528	940	51	400	970	106	0.777
168	1.83	80	90	528	940	51	400	970	106	0.924
169	1.83	120	60	528	940	51	400	970	106	0.534
170	1.83	120	0	528	940	51	400	970	106	0.432
171	1.83	120	90	528	940	51	400	970	106	0.548
172	2.02	40	60	528	940	51	400	970	106	1.207
173	2.02	40	0	528	940	51	400	970	106	0.938
174	2.02	40	90	528	940	51	400	970	106	1.241
175	2.02	80	60	528	940	51	400	970	106	1.095
176	2.02	80	0	528	940	51	400	970	106	0.764
177	2.02	80	90	528	940	51	400	970	106	1.135
178	2.02	120	60	528	940	51	400	970	106	0.548
179	2.02	120	0	528	940	51	400	970	106	0.535
180	2.02	120	90	528	940	51	400	970	106	0.662